Plant Biotechnology Journal
Open Access

Plant Biotechnology Journal (2022)**20**, pp. 1518–1532 doi: 10.1111/pbi.13830

Overexpression of cytoplasmic C_4 *Flaveria bidentis* carbonic anhydrase in C_3 *Arabidopsis thaliana* increases amino acids, photosynthetic potential, and biomass

Deepika Kandoi[1], Kamal Ruhil[1], Govindjee Govindjee[2] and Baishnab C. Tripathy[1,3,*]

[1]*School of Life Sciences, Jawaharlal Nehru University, New Delhi, India*

[2]*Department of Plant Biology, Department of Biochemistry, and Center of Biophysics & Quantitative Biology, University of Illinois at Urbana-Champaign, Urbana, IL, USA*

[3]*Department of Biotechnology, Sharda University, Greater Noida, UP, India*

Received 9 March 2021;
revised 15 April 2022;
accepted 18 April 2022.
**Correspondence* (Tel: +91 981 810 4924; fax: +91 120 232 3667; email baishnabtripathy@yahoo.com)

Keywords: *Arabidopsis thaliana*, carbonic anhydrase, C3 photosynthesis, C4 photosynthesis, CO_2 assimilation, Photosystem I, Photosystem II, water-use efficiency.

Summary

An important method to improve photosynthesis in C_3 crops, such as rice and wheat, is to transfer efficient C_4 characters to them. Here, cytosolic carbonic anhydrase (CA: *βCA3*) of the C_4 *Flaveria bidentis* (*Fb*) was overexpressed under the control of ^{35}S promoter in *Arabidopsis thaliana*, a C_3 plant, to enhance its photosynthetic efficiency. Overexpression of *CA* resulted in a better supply of the substrate HCO_3^- for the endogenous phosphoenolpyruvate carboxylase in the cytosol of the overexpressers, and increased its activity for generating malate that feeds into the tricarboxylic acid cycle. This provided additional carbon skeleton for increased synthesis of amino acids aspartate, asparagine, glutamate, and glutamine. Increased amino acids contributed to higher protein content in the transgenics. Furthermore, expression of *FbβCA3* in *Arabidopsis* led to a better growth due to expression of several genes leading to higher chlorophyll content, electron transport, and photosynthetic carbon assimilation in the transformants. Enhanced CO_2 assimilation resulted in increased sugar and starch content, and plant dry weight. In addition, transgenic plants had lower stomatal conductance, reduced transpiration rate, and higher water-use efficiency. These results, taken together, show that expression of C_4 *CA* in the cytosol of a C_3 plant can indeed improve its photosynthetic capacity with enhanced water-use efficiency.

Introduction

The current global research efforts are focusing on increasing crop yield for food and fuel production (Long *et al.*, 2015). C_3 photosynthesis is often limited by available CO_2 for ribulose bis phosphate carboxylase/oxygenase (*rubisco*). Therefore, it is important to modulate C_3 photosynthesis to enhance plant productivity. Carbonic anhydrase (CA, EC 4.2.1.1) is mostly a zinc-containing metalloenzyme that catalyses the inter-conversion of CO_2 and HCO_3^- and is widely distributed in both eukaryotes and prokaryotes (Badger and Price, 1994; Bonacci *et al.*, 2012; Hewett-Emmett and Tashian, 1996; Liljas and Laurberg, 2000; Momayyezi *et al.*, 2020; Moroney *et al.*, 2001). *CAs* belong to six independent gene families (Moroney *et al.*, 2011): *α-CAs*, *β-CAs*, *γ-CAs*, *δ-CAs*, *ε-CA* and *ζ-CA*. In higher plants, only *α-CA*, *β-CA*, and *γ-CA* exist. In spite of their structural differences, they share the same general catalytic mechanism (Lindskog, 1997). Amino acid sequence alignment of cytoplasmic C_4 *Flaveria bidentis βCA3* (*FbβCA3*), with different isoforms of C_3 *Arabidopsis thaliana βCAs* (*AtβCAs*), demonstrates that these sequences have similar binding sites for Zn^{2+} as well as for the substrates (see Figure S1). In addition, great deal is now known about the structure and varied functions of carbonic anhydrases in plants (DiMario *et al.*, 2017).

In C_3 plants, up to 2% of the total leaf protein is CA, and 95% of its activity is in chloroplast stroma (Okabe *et al.*, 1984; Tsuzuki *et al.*, 1985). Without the *CA*, the hydration of CO_2 is very slow (Raven, 1997). The role of various *CA* components in terrestrial C_3 plants in photosynthesis is less understood seemingly due to the compensatory effect of multiple *CA* isoforms (DiMario *et al.*, 2018). The C_3 isoforms of *CA* are involved in seed germination, lipid biosynthesis, morphogenesis, nodule of legumes, and responses to abiotic stress (Flemetakis *et al.*, 2003; Floryszak-Wieczorek and Arasimowicz-Jelonek, 2017; Hoang and Chapman, 2002; Kavroulakis *et al.*, 2000). The CO_2 usually diffuses from the cytoplasm to the chloroplasts either through the lipid bilayer or through the pores of aquaporins (Flexas *et al.*, 2008; Groszmann *et al.*, 2017; Tyerman *et al.*, 2002). For research on the transport of bicarbonate in plants and algae, see Poschenrieder *et al.* (2018). Furthermore, thylakoid CAs are involved in converting CO_2 to HCO_3^- in Photosystem II (DiMario *et al.*, 2016), where the latter is needed not only for binding on the non-heme iron for the functioning of electron flow for the reduction of plastoquinone but also for binding near manganese on the 'oxygen evolving complex' for water oxidation (Shevela *et al.*, 2012; Shitov *et al.*, 2018; Stemler, 1997). Without bicarbonate bound in Photosystem II, there is no photosynthesis.

In C_4 mesophyll cells, *CA* is known to catalyse the hydration of CO_2 producing HCO_3^-, (Hatch and Burnell, 1990), the latter being the substrate for phosphoenolpyruvate carboxylase (*PEPC*; Ludwig, 2012). C_4 plants are efficient in carbon assimilation and have an advantage over C_3 plants under several ecological conditions. In the past, there have been attempts to overexpress

(or regulate) C_4 pathway genes into C_3 plants (Borba *et al*., 2018; Kandoi *et al*., 2016, 2018; Lin *et al*., 2020; Miyao *et al*., 2011; Schuler *et al*., 2016; Sen *et al*., 2017). Although Hu *et al*. (2010) and Pal and Borthakur (2015) have succeeded in overexpressing C_3 *CA* in the cytosol, in chloroplasts, and in the guard cells of C_3 plants, no increase in the rates of photosynthesis was observed. Furthermore, Majeau *et al*. (1994) showed that the chloroplastic *CA* antisense plants compensate by increasing their stomatal conductance leading to an increase in water loss. In tobacco, antisense/mutant of chloroplastic *CA* that had substantial loss of *CA* produced no significant decrease in the rate of photosynthesis (Hines *et al*., 2021; Price *et al*., 1994). The seedling establishment was affected in chloroplastic *β*CA1-deficient *Arabidopsis* (Ferreira *et al*., 2008). The knockout of cytosolic *βca2* and *βca4* reduced *Arabidopsis* growth rates and caused chlorosis of the younger leaves, when grown at low [CO_2] due to reduction in amino acid biosynthesis (DiMario *et al*., 2016); further, *βCAs* gene expression and enzymatic activities are important for optimal plant growth (Dąbrowska-Bronk *et al*., 2016).

A pertinent question is whether overexpression of cytoplasmic C_4 CA, having higher affinity for CO_2 (Km = 0.8–2.8 mM) than that of C_3 *CA* (Km = 15–42 mM) (Hatch and Burnell, 1990; Ignatova *et al*., 1998; Pocker and Ng, 1973; Tobin, 1970), and its higher ability to hydrate CO_2, in the cytosol of C_3 plants, can increase amino acid content and photosynthetic efficiency. To explore this question, we have overexpressed carbonic anhydrase *βCA3* from *Flaveria bidentis* into *Arabidopsis thaliana* (Figure 1); we show here that this indeed leads to increased amino acid (aspartate, asparagine, glutamate and glutamine) content, improved photosynthesis (16%–22%), better water-use efficiency (22%–26%), higher starch content (10%–19%), and even higher biomass (14%–20%).

Results

Sequence alignment of *Flaveria bidentis βCA3* with *Arabidopsis thaliana βCA* isoforms

Six isoforms of *βCA* are present in *Arabidopsis thaliana*: three are cytosolic, two chloroplastic, and one mitochondrial. A comparison of the amino acid sequence of *Arabidopsis* with *Flaveria* cytosolic *βCA3* demonstrates homology of 57%–72% among cytosolic isoforms, 36%–58% in chloroplastic isoforms, and 33% in mitochondrial isoforms (Table S1); furthermore, the catalytic sites of the enzyme are highly conserved in the *AtβCAs* and in *FbβCA3* (Figure S1).

Transformation, genomic DNA analysis of transgenic plants

To overexpress cytoplasmic C_4 *CA* into C_3 plants, we cloned *FbβCA3* into a transformation vector pCAMBIA1304 (Figure 2a). Recombinant pCAMBIA1304: *FbβCA3* was then used for *Agrobacterium*-mediated *Arabidopsis* transformation to raise transgenic plants.

Genomic DNA was isolated from different transgenic *Arabidopsis* lines overexpressing *FbβCA3*, and then the *FbβCA3* was amplified by PCR using ^{35}S forward and *FbβCA3*-specific reverse primers that yielded a fragment of ~0.8 kb of *FbβCA3*, suggesting that the transgene had been integrated into the host genome (Figure S2a). To confirm the insertion of the binary vector, without the gene in vector control (VC) plants, kanamycin (*nptII*) gene was amplified by PCR, using *nptII*-specific forward and reverse primers. Our PCR results showed that a fragment of ~0.8 kb from the transformants contained *nptII* (Figure S2b). Plants of these confirmed individual transgenic lines were then grown to harvest seeds; these seeds were grown again in kanamycin plates to select T2 transgenic lines. Transgenic seeds were then grown to get T4 generations to obtain homozygous transgenic plants for further use.

Southern blot analysis

The number of integrations of the T-DNA cassettes containing *FbβCA3* cDNA in the *Arabidopsis thaliana* host genome was checked by Southern blot analysis, using the *nptII* probe. The transgenic lines CAx2, CAx3 and CAx5 showed single bands confirming single integration of the transgene into the *Arabidopsis* genome. However, the CAx6 line showed a double band, which implies that there was a two-time integration of the transgene into the host genome (Figure S2c). VCs showed the presence of a single copy of T-DNA cassette and, there was no band of *nptII* in the wild type (WT).

Phenotype of plants

Figure 2b shows a photograph of a four-week-old VC as well as that of CA overexpressed plants. Visually, plants of CAx3 and CAx5 transgenic lines show better growth than those of the VCs (see the last section of 'Results' for differences in growth, and weight of these plants).

Gene expression

The qRT-PCR analysis, using gene-specific primers, showed that the expression of the *FbβCA3* varied among the transgenic lines. The transcript abundance in CAx1, CAx3, and CAx5 was 1.3-, 1.8-, and 2.3-fold higher, respectively, compared with that in the CAx2 (Figure 2c).

Immunoblot analysis

To check changes in protein expression in the transgenics, we performed Western blot for proteins isolated from 4-week-old VC and *FbβCA3x* lines. Polyclonal antibodies raised against *FbβCA3* protein, as described in *Experimental Procedures*, were used to immuno-detect the CA protein in different *FbβCA3x* lines. In the transgenic lines, the abundance of CA protein (~28 kD) was higher than in the VCs (Figure 2d,e). The VC showed the expected band due to the high homology of *AtβCAs* with *FbβCA3*.

Enzyme activity of carbonic anhydrase

CA activity in VC was 276 μmol CO_2 hydrated (mg Chl)$^{-1}$ min^{-1}; however, this activity, in different transgenic lines, ranging from 348 to 550 μmol CO_2 hydrated (mg Chl)$^{-1}$ min^{-1}, was 1.3- to 2.0-fold higher than in the VCs (Figure 2f). Based on their higher transgene expression, protein abundance and enzymatic activity, CAx3, and CAx5 transgenic lines were selected for further studies.

Chlorophyll, free amino acids, and protein content

There was no significant difference in the Chl content, Chl *a*/*b* ratio, free amino acids and the total protein content of WT and VC plants (Figure 3a–d). The CAx3 and CAx5 transgenics had 11% to 15% higher total Chl than the WT and the VC plants

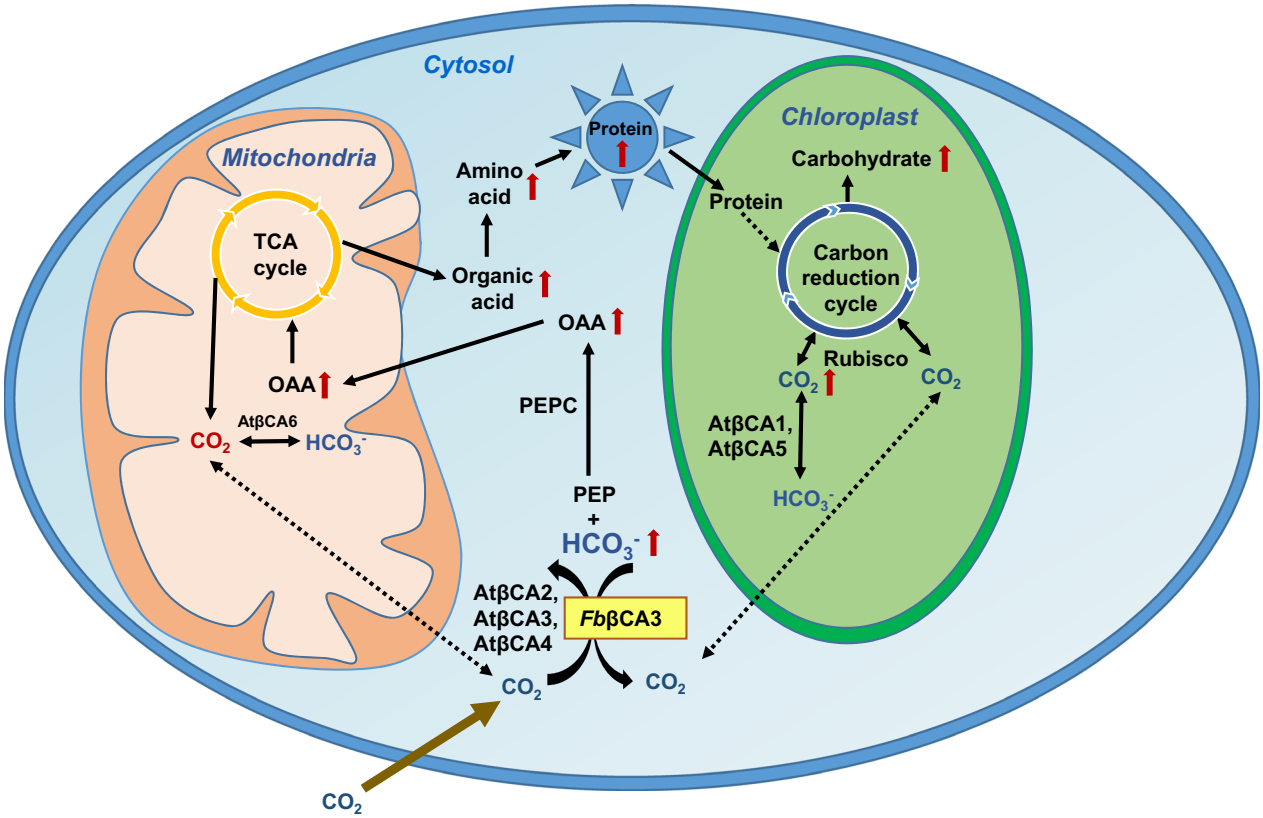

Figure 1 A proposed model of photosynthetic carbon flow in *Arabidopsis thaliana* overexpressing *FbβCA3*. The overexpressed cytosolic *FbβCA3*, having low Km for CO_2, increases the hydration of CO_2. The dashed arrows indicate the diffusion of CO_2 within the cytosol and the organelles. *FbβCA3* overexpression increases the flux of the carboxylic acid to the tricarboxylic acid (TCA) cycle in mitochondria and plays an anaplerotic role in synthesizing higher amounts of total amino acids and proteins that contribute to increases in photosynthetic efficiency and biomass (OAA- oxaloacetic acid; PEP- phosphoenolpyruvate; PEPC- phosphoenol pyruvate carboxylase; TCA cycle- tri carboxylic acid cycle).

(Figure 3a). However, the Chl *a*/*b* ratio was similar in the WT, VC and in the CA overexpressers (Figure 3b). Furthermore, as compared to WT and VC plants, the total free amino acids increased by 12% in CAx3 and 16% in CAx5 lines (Figure 3c). Similarly, the protein content of CAx3 and CAx5 was 10%–12% higher than in the WT and VC plants (Figure 3d). Therefore, for further analysis, we have compared the VC plants with the transgenics.

TCA cycle intermediates and amino acids

To understand whether the reason for higher protein content of transgenics is due to enhanced synthesis of amino acids and its carboxylic acid carbon precursors, the accumulation of certain carboxylic acids and amino acids was analysed by gas chromatography-mass spectrometry (GC-MS). Enhanced oxaloacetic acid (OAA) synthesis, due to increased *PEPC* substrate (HCO_3^-) availability in the transgenics, resulted in ~40% increase in malate accumulation (Figure 3e). Furthermore, fumarate also increased by 30% in the transgenics (Figure 3e). Similarly, the OAA-derived amino acids, such as aspartic acid and asparagine, increased much more, by 70%–80% in the transgenics (Figure 3f). In addition, glutamate and glutamine, derived from α-ketoglutarate, a TCA cycle component, increased by 12% and 18% respectively (Figure 3f), and alanine, derived from pyruvate, doubled in the transgenics (Figure 3f).

Enzyme activity of phosphoenolpyruvate carboxylase (PEPC)

In vitro assay of PEPC, where 10 mM sodium bicarbonate was exogenously added to the reaction mixture, showed its activity to be similar in the VC and transgenic plants (~3.45 μmol (mg protein)$^{-1}$ h^{-1}) (Figure S3).

Whole-chain, PSII, and PSI reactions

Under saturating light, and on Chl basis, thylakoids isolated from the *CA* overexpresser plants, as compared to that from the VC plants, showed higher (20%–28%) electron transfer rates for the whole chain (WC) reaction (Figure 3g). The partial reactions of PSII as well as of PSI increased by 21%–26% and 23%–32%, respectively, in the transgenics (Figure 3h,i).

Chlorophyll *a* fluorescence

To obtain further information on WC, particularly on PSII, we used Chl *a* fluorescence as its non-invasive signature. Various Chl *a* fluorescence parameters were measured as described under *Experimental Procedures*; these results are described below.

Rates of electron transport (ETR II and ETR I)

At saturating light intensity (540 μmol photons m^{-2} s^{-1}), the calculated values of ETR II and ETR I were higher by 13%–19%

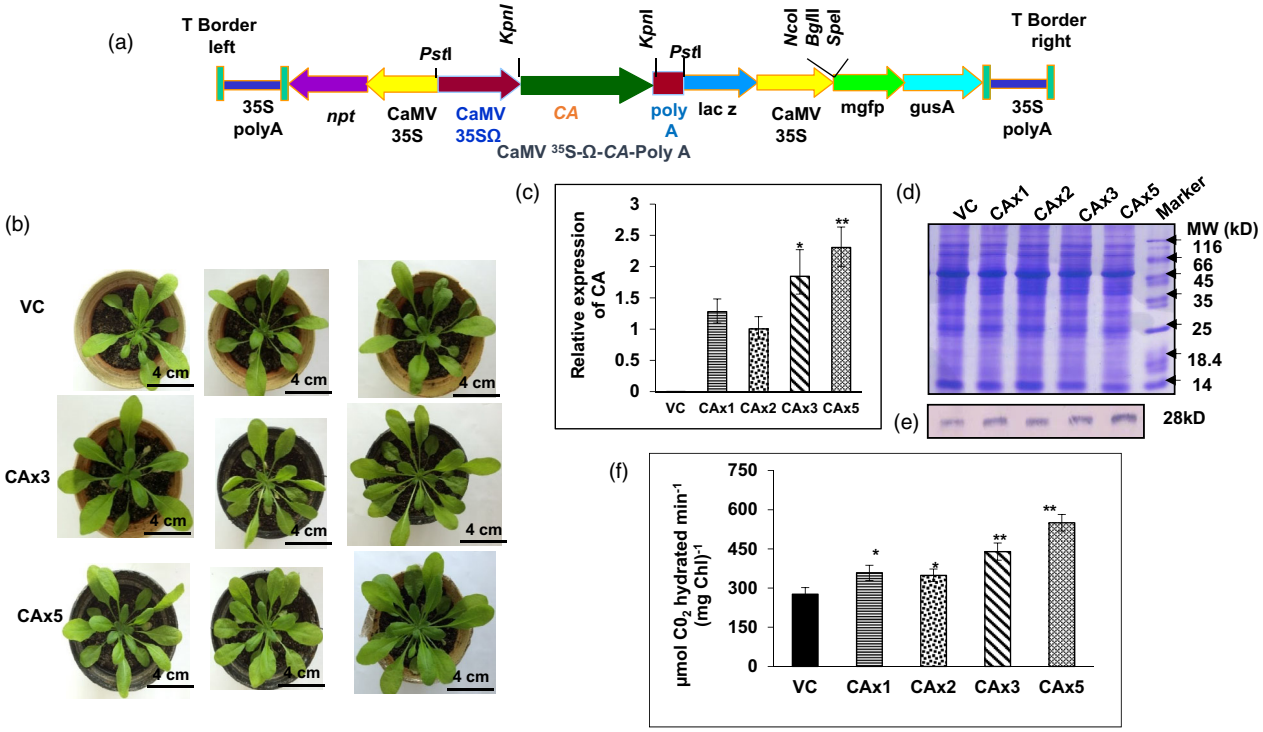

Figure 2 A schematic representation of the transgene used for *Arabidopsis* transformation, photographs, and confirmation of *Flaveria bidentis CA* overexpressed *in Arabidopsis*. (a): *Flaveria bidentis βCA3* cloned to pCAMBIA1304 vector having CaMV35S-Ω-poly A promoter cassette; CaMV35S-npt, coding region of neomycin phosphotransferase gene with CaMV35S promoter; CaMV35SΩ, CaMV 35S promoter with omega (Ω) enhancer; *FbβCA3* cDNA, coding region of *Fb*CA gene; Poly A, Poly A tail; (b): *Arabidopsis* vector control (VC) and *CAx* (CAx3 & CAx5) plants grown at 21 °C under 14h L/ 10 h D photoperiod in cool-white-fluorescent light (100 µmol photons m^{-2} s^{-1}) for 4 weeks in pots; (c): qRT-PCR of *FbβCA3*—relative gene expression of *CA* in VC and transgenic lines using CAx2 as a reference; (d): 15% SDS-PAGE: 25 µg of protein was loaded in each lane and SDS-PAGE was run to check the separation of the protein(s); (e): Western blot: protein samples from the gel were transferred to nitrocellulose membrane and immunoblot analysis of CA protein was made using *Flaveria bidentis* CA antibodies; (f): CA enzymatic activity: the activity of CA in VC was 276 µmol CO_2 hydrated (mg Chl)$^{-1}$ min^{-1}; it ranged from 348 to 550 µmol CO_2 hydrated (mg Chl)$^{-1}$ min^{-1} in different transgenic lines (CAx1, CAx2, CAx3 and CAx5; VC: vector control plants containing the null vector pCAMBIA1304). Each data point is the average of 3 replicates for 2c,f. The error bars for 2c is the standard error of the mean (SEM) and for 2f error bar represents ± SD; asterisks indicate significant differences determined by ANOVA-test with Dunnett's post hoc test compared to the controls (*$P < 0.05$, **$P < 0.01$).

and 17%–25%, respectively, in the transgenics than in the VC plants (Figure 4a,b).

Chlorophyll a fluorescence transient

For these measurements, OJIP curves were recorded up to 1 s, after excitation with 650 nm light of high intensity (3500 µmol photons m^{-2} s^{-1}), provided by an array of 3 LEDs. Different curves in Figure 4c are for Chl *a* fluorescence transients of dark-adapted leaves of *Arabidopsis thaliana*, plotted on a logarithmic time scale from 20 µs to 1 s; here, all the curves were normalized at 20 µs (taken to be Fo). Fluorescence transients of both VC and transgenic plants show typical OJIP curves; CAx3 and CAx5 show a similar fluorescence rise from O to J, but a faster rise from J to I and I to P as compared to those in the VC.

When we double-normalize the IP rise, that is, both at the I level (30 ms) as well as at the P level (290 ms) (see Figure 4d), we observe that the transgenic plants have a faster IP rise than the VC. Furthermore, when the OJIP curves are normalized at 'I' only, we observe a faster IP rise in the transgenics than in the vector controls (Figure 4e).

We now describe observations on quantitative differences between the VC and the transgenics on several key Chl *a* fluorescence parameters.

1. F_o, the initial minimum fluorescence: As compared to the VC, CAx3 and CAx5 plants have ~8% and ~11% higher values (Table S2), but this is simply due to higher [Chl] in the transgenics (Figure 3a) since there was no difference in the values of F_o/Chl.
2. F_m, the maximal fluorescence (see *Experimental Procedure*): The F_m values of CAx3 and CAx5 plants are higher by ~18% and ~25% (Table S2); furthermore, the F_m/Chl values are 6%–9% higher in the transgenics than in the VC.
3. F_v/F_m, an estimate of the maximum potential quantum efficiency of PS II: when all the reaction centres are open (i.e. when dark-adapted samples are used), this ratio increased only slightly (~5%) in the transgenic plants (Table S2).
4. *Area over the OJIP curve*, an area between F_o and F_m, which is proportional mainly to the size of the plastoquinone pool (Malkin and Kok, 1966): It was clearly higher (19%–22%) in CAx3 and CAx5 than in the VCs (Table S2).
5. F_v/F_o, reflecting the efficiency of the (electron) donor side of PSII (Burke, 1990): It was higher (11%–16%) in the transgenics than in the VCs (Table S2).
6. *PI, the performance index* (see Tsimilli-Michael *et al*., 2000): It was higher (10%– 20%) in the transgenics than in the VCs (Table S2).

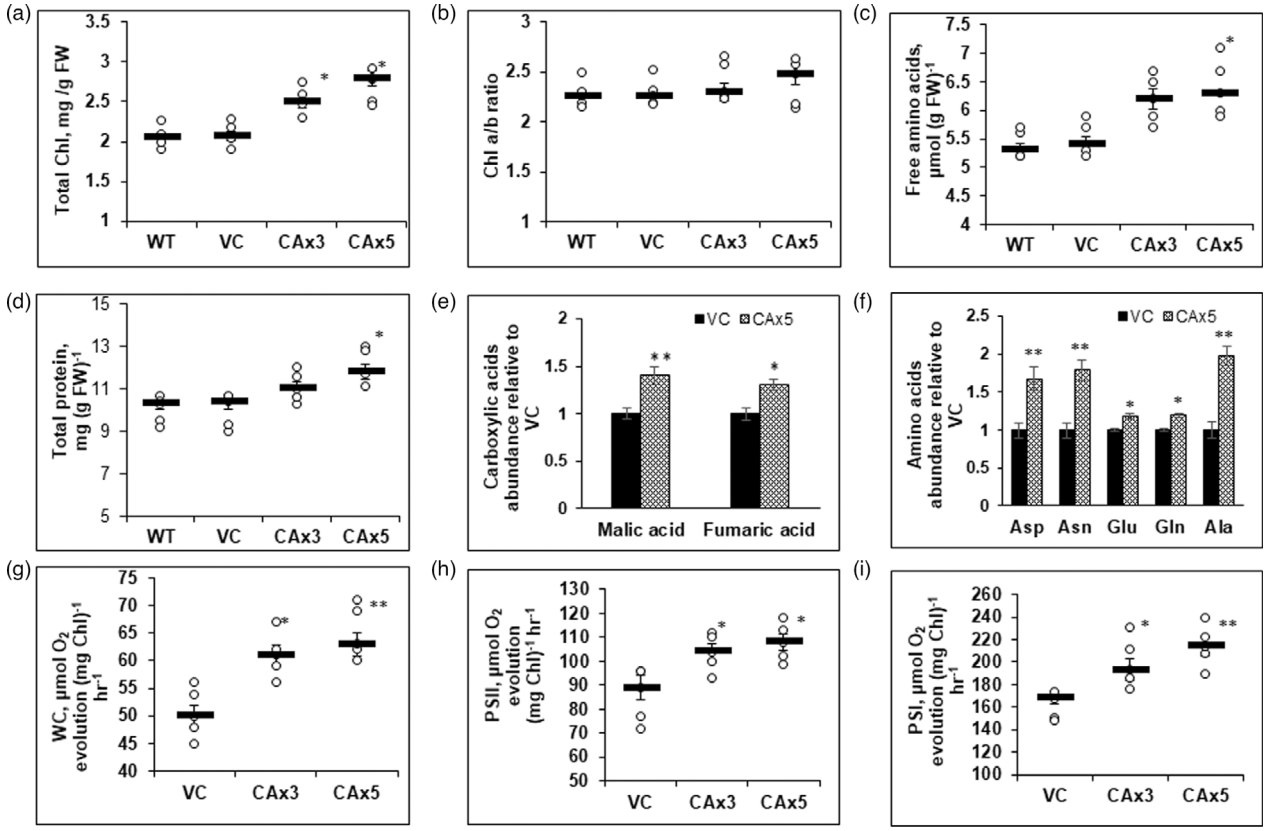

Figure 3 Total chlorophyll (Chl), Chl *a*/b ratio, free amino acids, total protein, metabolite assay and electron transport reactions. (a): Total chlorophyll (Chl) content; (b): Chl a/b ratio; (c): Free amino acids; (d): Total protein content; (e) and (f) Carboxylic acid abundance and amino acids abundance in CAx5 relative to the internal standard (ribitol); VC was taken as 1; (g): Electron transport through the whole chain, both PSI & PSII (water to methyl viologen; oxygen uptake); (h): Electron transport through PSII (oxygen evolution; water to phenylenediamine); (i): Electron transport through PSI (ascorbate to methyl viologen; oxygen uptake). VC: vector control; and 2 different transgenic lines, CAx3 and CAx5. Each data point is the average of five replicates for 3a–d and 3g–l, and three replicates for 3e,f. The error bars represent ± SE; asterisks indicate significant differences determined by ANOVA-test (**P* < 0.05, ***P* < 0.01).

7. *Non-Photochemical Quenching (NPQ) of the excited state of Chl*: This parameter, which increases with light intensity, was lower (5%–9%) in CAx3 and CAx5 than in the VCs at 540 µmol photons m^{-2} s^{-1} (Figure 4f).

Gene expression

1. Expression of chlorophyll biosynthesis genes: (i) In comparison with the VC, *PBGS* (porphobilinogen synthase) was 1.7- and 2.2-fold higher in CAx3 and CAx5 (Figure 5a). (ii) The transcript expression of *UROD* (uroporphyrinogen decarboxylase), responsible for the synthesis of coproporphyrinogen, was 2.0- and 2.2-fold higher in CAx3 and CAx5 than in the VCs (Figure 5a). (iii) The gene expression of *PPOX* (protoporphyrinogen oxidase), responsible for protoporphyrin IX synthesis, increased 1.4–3-fold in the transgenics (Figure 5a). (iv) Furthermore, protoporphyrin-IX Mg-chelatase (*CHLI*), one of the 3 genes responsible for Mg insertion to protoporphyrin IX moiety, increased by 1.4- and 1.5-fold in CAx3 and CAx5, compared with that in the VCs (Figure 5a). (v) The expression of light-inducible protochlorophyllide oxidoreductase (*PORC*) was 1.8–2.5-fold higher in the transgenics than in the VC plants (Figure 5a).
2. Expression of photosynthesis-related genes: (i) The gene expression of *Lhcb1* and *Lhcb2.1*, encoding components of LHCIIs, was 2.1–2.5 and 1.9–2.5-fold higher in the transgenics (Figure 5b). (ii) The gene expression of *Lhca1* and *Lhca2*, encoding components of LHCIs, increased by 2–3.45- and 1.2–1.4-fold in the overexpressers (Figure 5b). (iii) Expression of *PsbA* and *PsbD*, encoding PSII's D1 and D2 proteins, was 3.2–3.6- and 1.7–2.3-fold higher in the transgenics (Figure 5b). (iv) *PsbO* (encoding for OEC33, the oxygen-evolving complex) increased, as compared to that in the VC plants, by 1.4- and 2.4-fold in CAx3 and CAx5 as compared to VC (Figure 5b).

Western blots of electron transport chain components

To ascertain if increased gene expression resulted in higher protein abundance in the transgenics, proteins of certain gene products were analysed by immunoblot. Besides, other photosynthetic proteins, that is, those involved in Chl biosynthesis, light harvesting, photosynthetic electron transport chain, and rubisco were analysed by Western blot (Figure 5c).

The images of Western blots revealed the abundance of UROD; LHCII, light-harvesting Chl-binding proteins, associated with PSII; PsbO, an oxygen evolving complex protein OEC33; inter-system electron transport component between PSI and PSII, that is, $Cytb_6f$ complex, and Cyt f; electron transport proteins of PSI, PsaE (PSI subunit IV); both the rubisco subunits (SU), the large (LSU) as

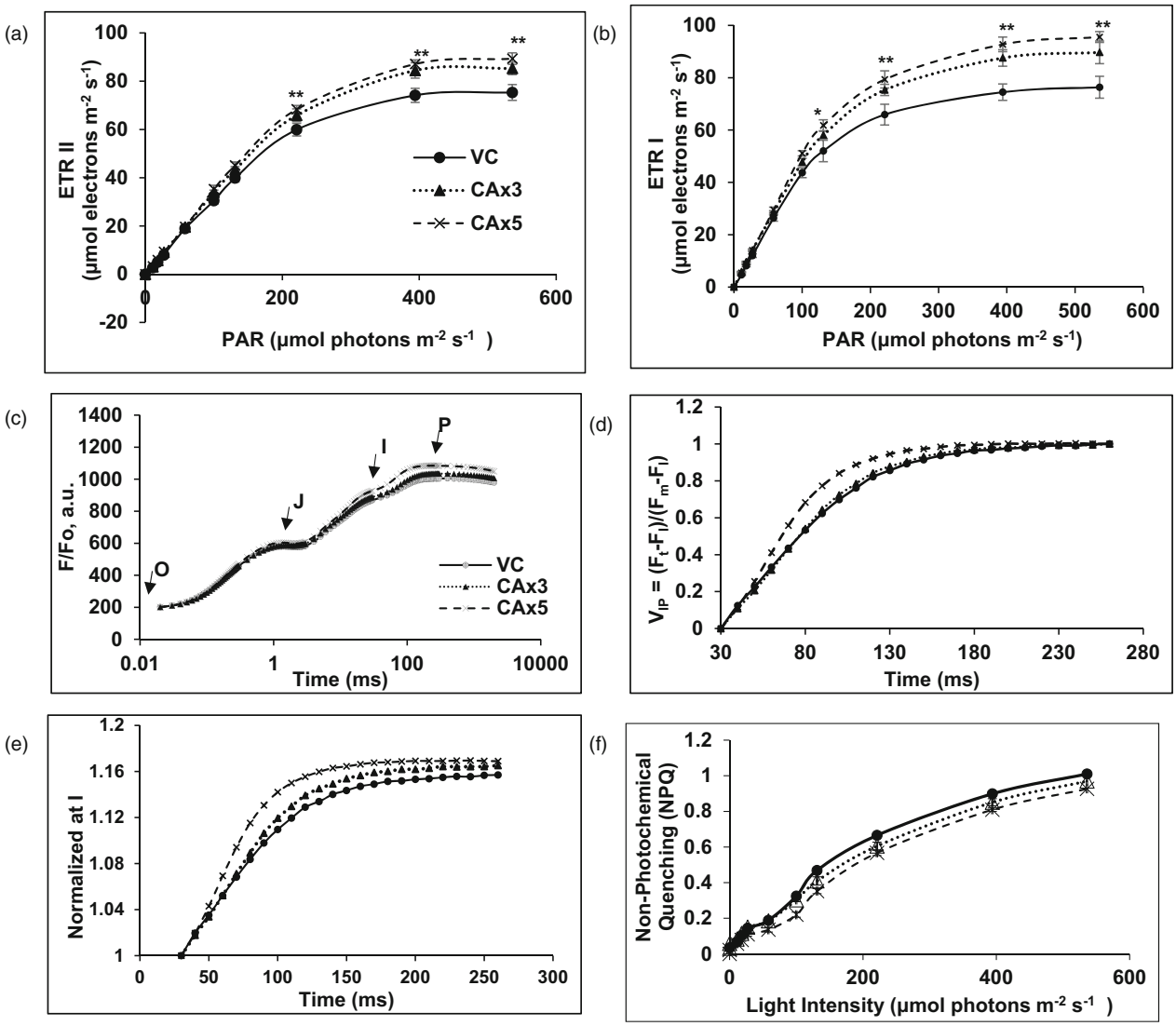

Figure 4 Electron transport reactions, the OJIP curves of chlorophyll *a* fluorescence and the non-photochemical quenching (NPQ) of the excited state of chlorophyll *a* of the vector control and *FbβCA3x* plants grown in soil. (a): ETRII; (b): ETRI; (c): Chl *a* fluorescence transients, with the OJIP curves normalized at the O level; (d): Variable fluorescence transients from the I to the P—double normalized between I (F_I) and P (F_p): $V_{IP} = (F_t–F_I)/(F_P–F_I)$; (e): Variable fluorescence transients from the I –single normalization; F, in the diagram, stands for fluorescence at time t (F_t), and F_o is for fluorescence at the O level; (f): NPQ of the excited state of chlorophyll at different light intensities. Each data point is an average of five replicates for 4a, b, and f and average of 8 replicates for 4c, d, and e; error bars represent ± SE.

well as the small (SSU), increased in the *CA* overexpressers (Figure 5c).

Light response curves for photosynthesis

Figure 6 shows the photosynthetic light response curves of the attached leaves, of both VC and the transgenics, as measured by IRGA (LiCOR-6400/XT), using 6400-18A RGB (red, green, blue) light source under ambient CO_2 (400 µmol/mol) and ambient O_2 (21%). At saturating light intensity (800 µmol photons m^{-2} s^{-1}), leaves of CAx3 and CAx5 had 17% and 23% higher net CO_2 assimilation rate, than in the VC plants (Figure 6a). The rate of respiration in the leaves of transgenics, as compared to the vector control, was also higher (~12%–16%) (Figure 6a,b). The quantum yield of CO_2 fixation, as measured at limiting-light intensities (up to 80 µmol photons m^{-2} s^{-1}) was 0.0423 in VC plants; it was higher by ~18% in CAx3 and CAx5 (Figure 6b). [We note that while calculating the quantum yield of CO_2 fixation, data at very low light intensity (10 µmol photons m^{-2} s^{-1}) were excluded from the regression analysis to avoid mixing it with the Kok effect, that is, inhibition of respiration by light (Sharp *et al.*, 1984).]

Stomatal conductance (g_s) and water-use efficiency (WUE)

The CO_2 assimilation rate, measured at 400 µmol photons m^{-2} s^{-1}, was 16% and 22% higher in CAx3 and CAx5 than in the VCs (Figure 6c). We note that the increased photosynthetic rate was associated with decreased stomatal conductance and transpiration rates in the transgenics. Stomatal conductance decreased by 10%–16% in the transgenics, as compared to that in the VC plants (Figure 6d); in addition, the transpiration rate decreased by ~7% in the *FbβCA* overexpressers (Figure 6e). Therefore, the water-use efficiency, the ratio of the CO_2

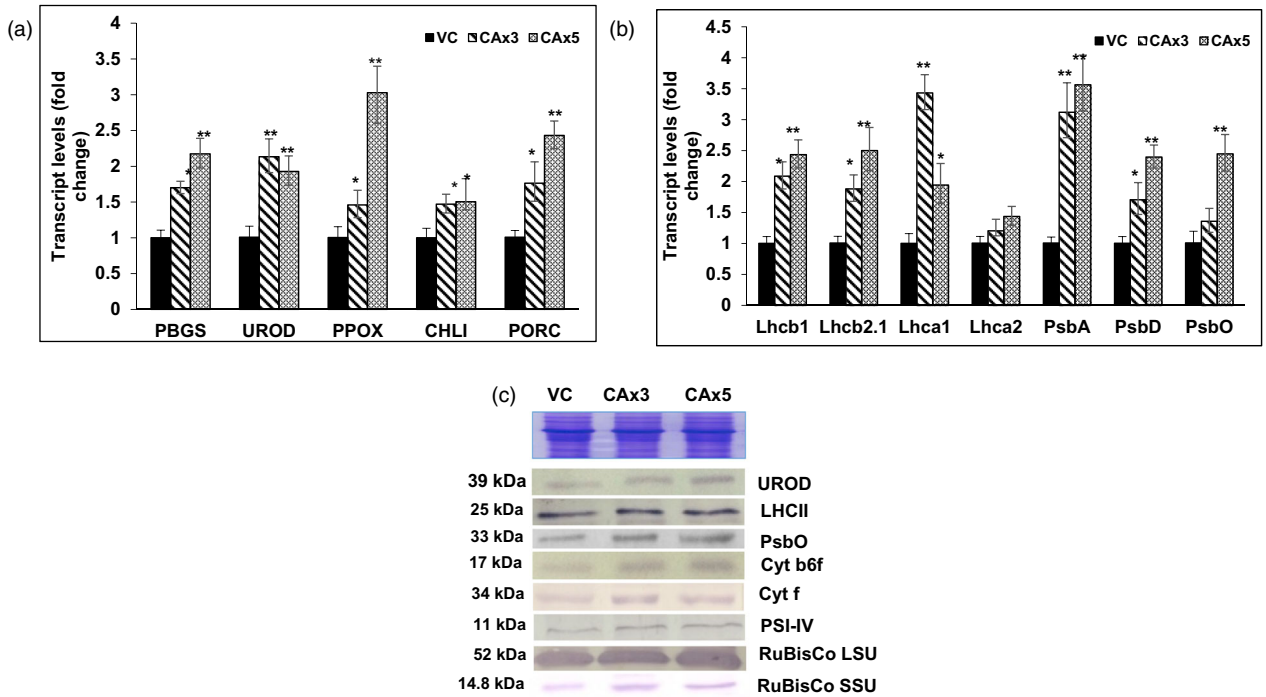

Figure 5 Relative gene expression and immunoblot analysis. Relative expression of genes related to (a): Chlorophyll biosynthesis; (b): Photosynthesis; (c): SDS-PAGE (12.5%) of protein (25 μg) isolated from VC and transgenic plants to check the separation of the proteins and the immunoblot to check the abundance of electron transport chain components. *Abbreviations*: *PBGS*: porphobilinogen synthase; *UROD:* encoding uroporphyrinogen decarboxylase; *PPOX1*: encoding protoporphyrinogen oxidase; *CHLI*: encoding protoporphyrin-IX Mg-chelatase; *PORC*: encoding the light-inducible protochlorophyllide oxidoreductase; *Lhcb1* and *Lhcb2*, encoding components of the light harvesting complex associated with PSII; *Lhca1* and *Lhca2*, encoding components of the light harvesting complex associated with PSI; PsbA and PsbD, core proteins, encoding Photosystem II D1 and D2 proteins; *PsbO*, encoding for OEC33, the oxygen-evolving complex; LHCII: light-harvesting chlorophyll-binding proteins; $Cytb_6f$ and Cytf, psaE- PSIIV; rubisco LSU and SSU: rubisco large and small subunits. qRT-PCR data are expressed as the mean ± SE of three independent experiments performed in triplicate. Asterisks indicate significant differences determined by ANOVA along with Dunnett's post hoc test compared to control (*$P < 0.05$, **$P < 0.01$).

assimilation rate to the transpiration rate (μmol CO_2 m^{-2} s^{-1}/ mmol H_2O m^{-2} s^{-1}), was higher by 22% and 26% in CAx3 and CAx5 than that in VC (Figure 6f).

A/C_i, Carbon assimilation rates and intercellular CO_2

In order to evaluate the contribution of photorespiration, *A*/C_i curves, under 21% and 2% oxygen, were measured (Figure 7a). In 21% O_2, the transgenic plants had higher photosynthetic capacity (the maximum rate of photosynthesis under CO_2 saturation at saturating light) than the VC plants. At saturating C_i (~1000 ppm), CO_2 assimilation rate increased by ~19% in CAx3 and ~22% in CAx5 transgenics as compared to the VCs (Figure 7a). Under 21% O_2, the carboxylation efficiency (*CE*), the initial slope of *A*/C_i curve (i.e. between 50 and 200 μmol mol^{-1} CO_2), in VC was 0.038 mol m^{-2} s^{-1}, which increased (by ~17%) to 0.044 mol m^{-2} s^{-1} in the transgenics. Further, there was no significant difference in the CO_2 compensation point of the VC and the transgenics. Similarly, the V_{cmax} (cf. Bernacchi *et al*., 2001) was 34 μmol m^{-2} s^{-1} for VC, which increased to 40 μmol m^{-2} s^{-1}, that is, by ~18% in transgenics. The electron transport rate J_{max} was 67 μmol m^{-2} s^{-1} in the VC, and it was higher by ~18%, that is, 84 μmol m^{-2} s^{-1} in the overexpressers. At higher CO_2 concentration, the *A*/C_i curve was parallel to the *X*-axis suggesting that the VCs and the transgenics may have limitation in triose phosphate utilization (Sharkey *et al*., 2007).

In 2% oxygen, the maximum rate of CO_2 assimilation, at saturating CO_2, was similar to that under 21% O_2 in all plants. However, the net CO_2 assimilation was 22%–25% higher in the transgenics than in the VCs. The carboxylation efficiency (CE) significantly increased with the decrease in the O_2 level, from 21% to 2%. The *CE* in VC was 0.045 mol m^{-2} s^{-1} but, it was 0.054-0.056 mol m^{-2} s^{-1} (higher by 19%–23%) in the transgenics under 2% O_2.

Mesophyll conductance (g_m) and chloroplast CO_2 concentrations (*Cc*)

In 6-week-old VC plants, leaf g_m, estimated from the combined gas exchange and other parameters, was 0.064 mol CO_2 m^{-2} s^{-1} bar^{-1}. In the two transgenics, g_m increased to 0.073 or 0.084 mol CO_2 m^{-2} s^{-1} bar^{-1}. However, these g_m values were comparatively lower in the VC as well as in the transgenics since the experiments were done on six-week-old plants (Flexas *et al*., 2007). Although there are problems in accurately measuring g_m in *Arabidopsis* leaves, because of their small size, we consistently observed increases in g_m in the transgenics. Similarly, using Thomas Sharkey's *A*/C_i curve fitting model (Sharkey *et al*., 2007), the g_m values had a similar pattern (15%–22% increase) in the overexpressers. However, this model did not predict a significant increase in the *Cc*s of the transgenics.

Growth, weight, sugar and starch content

The up-regulation of any functionally indispensable gene product (s) usually results in alterations in the development of the plant. We compared the overall growth of 3-week-old VC, CAx3, and

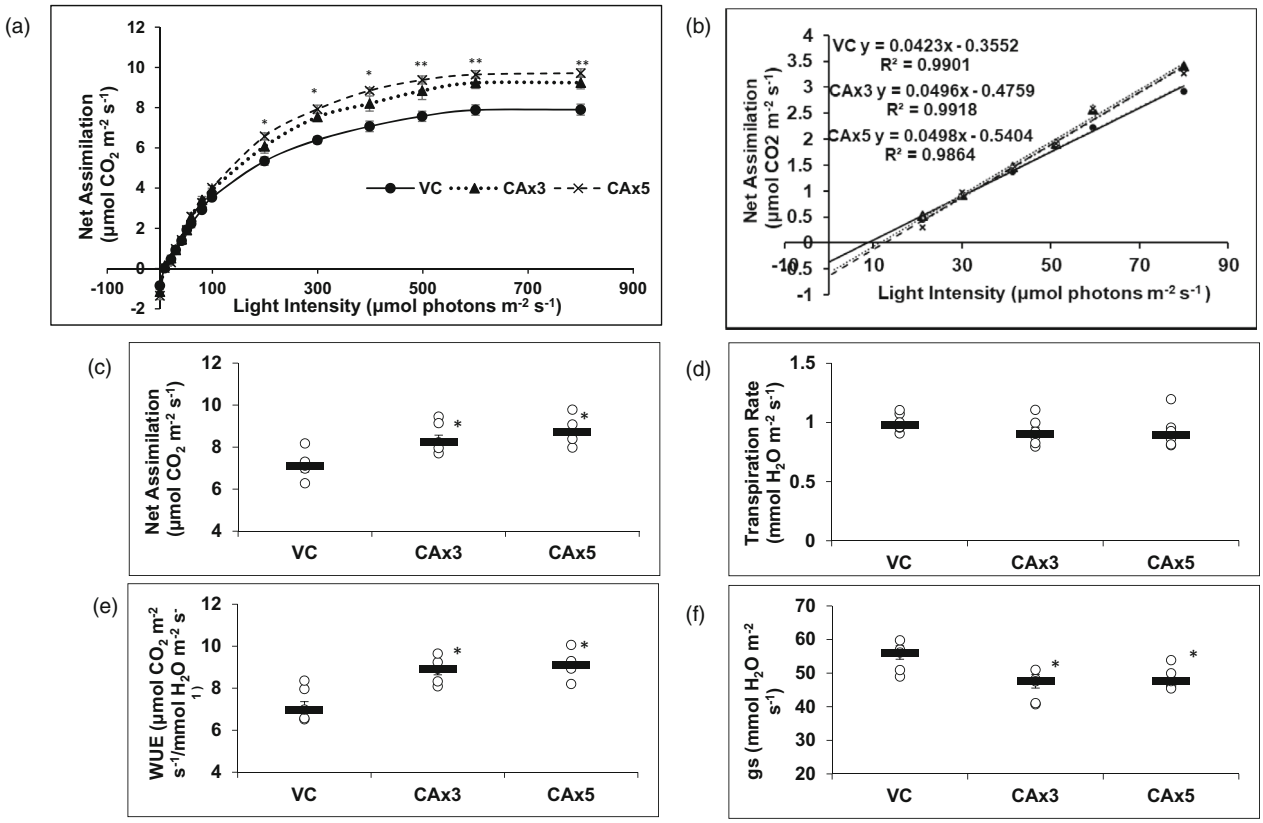

Figure 6 Photosynthesis (net CO_2 assimilation rate) light response curve. (a): Net CO_2 assimilation rates of vector control and *CAx* plants were monitored by IRGA (LiCor-6400/XT) in ambient CO_2 at 400 µmol photons m^{-2} s^{-1}, at 21 °C; (b): Net CO_2 assimilation rates up to 80 µmol photons m^{-2} s^{-1}; (c): Net CO_2 assimilation rates at 400 µmol photons m^{-2} s^{-1}; (d): Stomatal conductance (g_s); (e): Transpiration rate; (f): Water-use efficiency (WUE) of vector control and transgenic *Arabidopsis* plants. Each data point is an average of five replicates and error bars represent ± SE. Asterisks indicate significant differences determined by ANOVA with Dunnett's post hoc test (*$P < 0.05$).

CAx5 plants: both the overexpressers had longer (~14%) roots than in the VC plants (Table S3). Although their shoot lengths were almost similar (Table S3), they had larger (11%–15%) rosette diameter than in the VC plants (Table S3). After 3 weeks of growth, the dry weight of CAx3 and CAx5 plants increased by 14%, and 20%, respectively, as compared to VC plants (Figure 7b). Furthermore, increased photosynthetic carbon assimilation in the transgenics resulted in higher sugar and starch content. The content of glucose, fructose, and sucrose increased by 100%, 34%, and 19% in CAx5 plants respectively (Figure 7c). Similarly, the starch content of the leaves, harvested before dusk, increased by 10%–19% (Figure 7d).

All the above results clearly show that the transgenics had higher carboxylic acids, amino-acids, proteins, photosynthesis, carbohydrate, and biomass content than the VCs.

Discussion

We have generated *Arabidopsis thaliana* lines overexpressing C_4 *Flaveria bidentis βCA3* with higher affinity for CO_2. Overexpression of C_4 *FbβCA3* under the control of ^{35}S promoter resulted in higher gene expression, protein abundance, and enzymatic activity of *CA*, in the transgenic lines (Figure 2c,f,g). The expression of a transgene in the chloroplast usually results in higher level of transgene expression (Daniell *et al.*, 2001, and Lee *et al.*,2003).

Silencing of cytosolic *βCA2* and *βCA4* that decreased the carbon skeleton pool substantially reduced the aspartate, glutamate, and glutamine content in *Arabidopsis thaliana* (DiMario *et al.*, 2016). One of the reasons is that *PEPC* in the cytoplasm uses HCO_3^- to generate 50% of the aspartate in leaves (Melzer and O'Leary, 1987). The aspartate content was reduced to about two-thirds by the knockdown of PEPC (*Osppc4*) in rice (Masumoto *et al.*, 2010). Conversely, our data demonstrate that increased *CA* activity resulted in higher aspartate in the transgenics. The aspartate and its derivative asparagine increased by 70%–80% (Figure 3f). Similarly, glutamate and glutamine synthesized from the enriched supply of TCA cycle intermediate oxoglutarate also increased (10%–17%) in the transgenics (Figure 3d). Increased amino acid synthesis was due to the increased supply of carbon skeleton by TCA cycle intermediates, that is, OAA and oxoglutarate. We observed 40% increase of malate (Figure 3e), generated by the reduction of OAA by malate dehydrogenase (*MDH*). Furthermore, fumarate, another TCA cycle intermediate, increased by 30% (Figure 3e).

The increased availability of amino acids resulted in higher protein content in the transgenics (see Figure 1). Although Chl and proteins are synthesized via two different metabolic processes, their biosynthetic pathways are co-regulated by the nitrogen status of the plant (Garai and Tripathy, 2018). We propose that higher Chl content in the transgenics must have been due to increased expression of Chl biosynthetic genes,

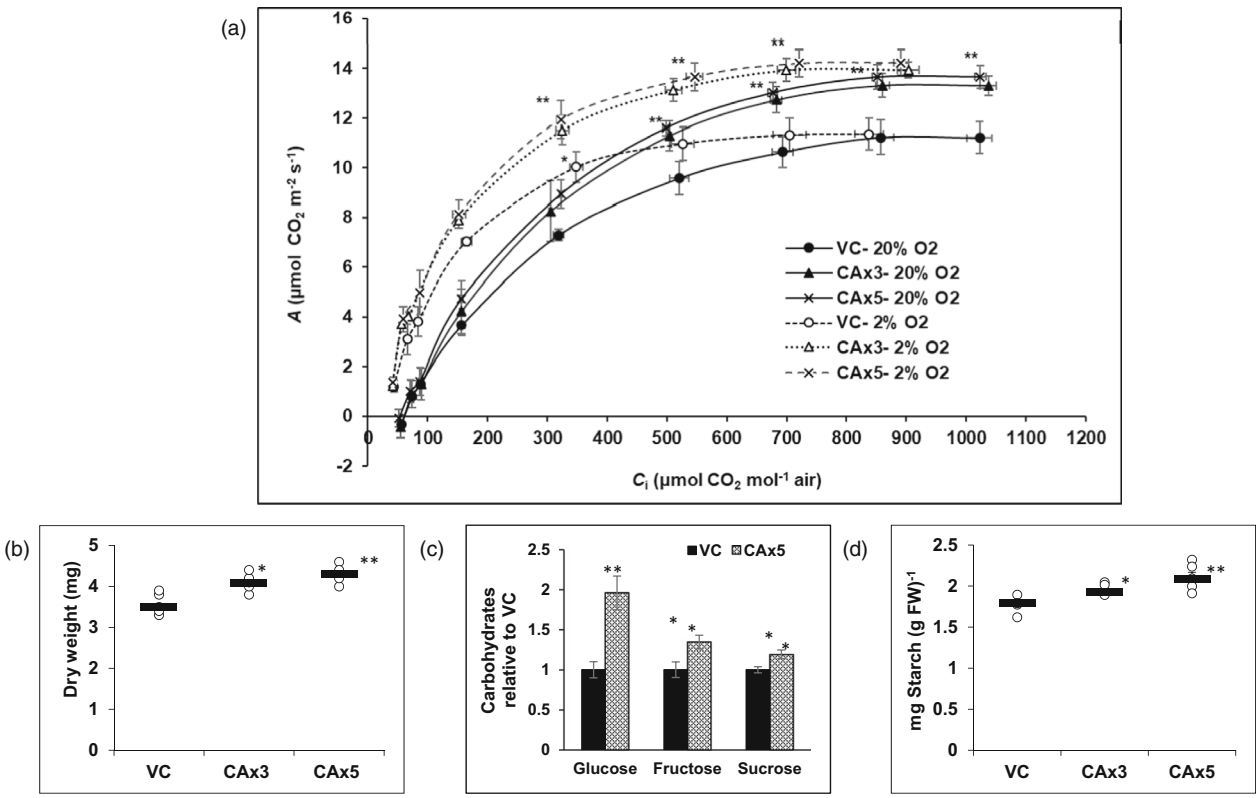

Figure 7 Photosynthetic carbon fixation rate as a function of increasing intercellular [CO_2] at 21% O_2 and 2% O_2 and carbohydrate content. (a): A/C_i curve; (b): Dry weight; (c): Saccharides in CAx5 relative to the internal standard (ribitol) and VC has taken 1; (d): Starch content, per g fresh weight (FW). Each data point is an average of five replicates and error bars represent SE. Asterisks indicate significant differences determined by ANOVA with Dunnett's post hoc test (*$P < 0.05$).

PBGS, *UROD*, *PPOX*, *CHLI*, and *PORC* (Figure 5a). Our results demonstrate the anaplerotic impact of *FbβCA3* overexpression on transcript abundance of genes involved in Chl biosynthesis.

Chlorophyll *a* fluorescence and photosystem activities in the trangenics

Chl *a* fluorescence has been used as a non-invasive signature of photosynthesis, particularly of PSII (Baker, 2008; Krause and Weis, 1991; Papageorgiou and Govindjee, 2004). When a dark-adapted photosynthetic organism is exposed to blue light (λ- 460 mm), Chl *a* fluorescence rises from a low initial minimum level (F_o) to a high level (F_m). The *CA* overexpressers had higher F_o (Table S2) likely due to higher Chl content. The maximum primary photochemical efficiency of PSII (Baker *et al*., 2007; Genty *et al*., 1992), based on F_v/F_m, was ~5% higher in the transgenics.

Higher photosynthetic efficiency in the transgenics

The increased ETR of PSII and PSI at low light (50–125 {mol photons m^{-2} s^{-1}) in *CA* overexpresser plants may be due to the availability of more photons absorbed by the larger antenna, and the latter may be due to increased gene/protein expression of light harvesting components of PSII and PSI: *Lhcb2.1*, LHCII, *Lhcb1*, *Lhca1*, and *Lhca2* (Figures 5b,c and S5). ETR at high light (~550 {mol photons m^{-2} s^{-1}) was also higher (13%–19% for PSII; 17%–25% for PSI) in *CAx* plants than in the VC (Figure 4a, b), consistent with light-saturated PSII, whole-chain and PSI rates in isolated thylakoid membranes (Figure 3g–i). We suggest that higher light-saturated PSII- and PSI-dependent ETR in the leaves, and higher PSII and PSI activities of thylakoid membranes, from the transgenics, are due to the increased gene expression/protein abundance of *PsbA*, *PsbD*, *PsbO*, PsaE, $Cytb_6f$ complex, and other proteins. We conclude that the *CAx* plants have (i) a higher light-harvesting capacity under limiting light due to larger antenna and (ii) a greater ability to use high light due to more and efficient PSII, PSI, and intersystem ETCs. Also, OEC33, on the electron donor side of PSII, has CA activity (Lu *et al*., 2005). Thus, higher OEC33 in the transgenics may have led to enhanced PSII-dependent ETR, under high light. Coupled with higher PSI and PSII reactions, increased cytochrome b6/f complex may have contributed to higher WC activity in the transgenics. For other systems, see Biswal *et al*. (2012) and Simkin *et al*. (2017). Further, PsaE (PSIIV, Figure 5c), involved in PSI cyclic electron transport, which prevents electron leakage to O_2 (see Jeanjean *et al*., 2008), was increased in *CAx* plants; thus, this may have minimized the photoreduction of ROS by PSI.

In the Chl *a* fluorescence induction (OJIP) curve, normalized at the 'O' level (F_o), we observe, in the transgenics, a faster JI rise as well as a faster IP rise; this may be due to higher efficiency of electron transport in the transgenics (Figure 4c; cf. Kandoi *et al*., 2016; Jiménez-Francisco *et al*., 2020). The faster IP rise in the transgenics suggests higher photosynthesis efficiency (cf. Hamdani *et al*., 2015; Soda *et al*., 2018), consistent with their higher 'performance index'. The area over the OJIP curve, between F_o and F_m, proportional to the size of the pool of the electron acceptors in PSII (Malkin and Kok, 1966), was higher (19%–22%) in the CAx3 and CAx5 than in the VC plants (Table S2), confirming the advantage of the transgenics over the controls.

Carbon fixation and water-use efficiency (WUE)

The rate of CO_2 fixation measures the performance of plants. We demonstrate here that overexpression of *FbβCA3* resulted in higher rates of photosynthetic carbon assimilation, per unit leaf area, than in the VC plants (Figure 6a). In the transgenics, the quantum yield of CO_2 assimilation, measured in limiting light intensities, other than at 10 μmol m^{-2} s^{-1} (to minimize Kok effect; Sharp *et al.*, 1984; Figure 6b), increased by ~18%. Thus, the transgenics had higher photosynthetic efficiency and they utilized the absorbed light energy much more efficiently.

Leaf is critical for transpiration, and vascular water transport sets limits on growth and drought tolerance. Our results demonstrate that the overexpression of *FbβCA3* in *A. thaliana* led not only to higher photosynthesis but also to lower stomatal conductance, decreased transpiration, and a better WUE (Figure 6d–f). Although the overexpression of *βCA1* or *βCA4* in the guard cells resulted in better WUE, there was no increase in photosynthesis rates (Hu *et al.*, 2010), showing the key role of *CA* in mesophyll cells. The overexpression of *FbβCA3* could, indeed, produce enough HCO_3^- under ambient CO_2 to partially close stomata to reduce the stomatal conductance and transpiration rate and, thus, increase the WUE. Our results further demonstrate that for efficient photosynthetic performance, relatively high *CA* activity is one of the important requirements in *A. thaliana*. For results on other systems where reduced CA activity leads to reduced photosynthesis and higher stomatal conductance, see von Caemmerer *et al.* (2004), Cousins *et al.* (2006); Osborn *et al.* (2017), Kolbe *et al.* (2018) and Ogée *et al.* (2018).

CO_2 response curves

CO_2 response curves provide crucial information on the photosynthetic capacity of plants at varying levels of CO_2. A typical response of light-saturated CO_2 assimilation rate (*A*) to leaf intercellular CO_2 mole fraction (C_i) has three phases: (i) when assimilation is limited by active *rubisco* (slope of the initial phase); (ii) when A_{max} is reached due to limitation by the supply of RuBP; and (iii) when there is no increase in carbon assimilation with increasing [CO_2], or to increasing [O_2], or when the system is limited by triose-phosphate utilization (Ainsworth and Long, 2005; Bernacchi *et al.*, 2013; von Caemmerer and Farquhar, 1981; Sharkey, 1985; Sharkey *et al.*, 2007). In 21% O_2, the transgenics had higher *A*, *CE*, V_{cmax}, and g_m than the vector control. Higher g_m may improve photosynthetic efficiency and intrinsic water-use efficiency (Flexas *et al.*, 2013). Increase in *CE* and V_{cmax} in the transgenics suggests that at the atmospheric [CO_2], the higher rates of photosynthesis is predominantly due to the anaplerotic role played by overexpressed CA that enhanced carboxylic acids, amino acids and protein content of plants (Figure 3d–f). The protein content of the leaves increased in the *FbβCA3* overexpressers. Since nearly half of the leaf protein is in *rubisco*, it is highly likely that transgenics had relatively higher *rubisco* content (Majeau *et al.*, 1994, and Majeau and Coleman, 1994), resulting in increased *CE*. Furthermore, V_{cmax}/*CE* has been shown to correlate with the amount of *rubisco* (von Caemmerer and Farquhar, 1981; Jacob *et al.*, 1995; Makino *et al.*, 1994; Manter and Kerrigan, 2004).

The CO_2 compensation point was almost similar both in the VC and in the transgenic plants and hence the rate of photorespiration did not decrease in the *CA* overexpressers. The increase in V_{cmax} and RuBP regeneration, in the transgenics, probably was partly due to a general increase in the protein content of leaves. The transgenics could recapture photorespiratory CO_2 by the efficient *FbβCA3* present in their cytoplasm. Under 2% O_2, photorespiration is expected to be minimal. Extrapolation of the A/C_i curve at 2% O_2 shows the CO_2 compensation point to be at ~7 μmol mol^{-1} (Figure 7a). Furthermore, the A/C_i curve in both the VC and the transgenics saturated at ambient CO_2; however, the *CE* of the transgenics was higher than that of the VC plants. The increases in *CE* and in the maximum rates of photosynthesis, under ambient CO_2, in the transgenics was clearly due to an increase in the inherent efficiency of photosynthesis. Under 2% O_2, the maximum rate of CO_2 assimilation is the same as under 20% oxygen, indicating that starch and sucrose synthesis set a ceiling on the rate of photosynthesis. This ceiling is higher in the plants with extra *CA*.

Due to their higher photosynthetic efficiency, the content of carbohydrates (glucose, fructose, sucrose and starch) was substantially higher in the transgenics (Figure 7c,d). The dark respiration is an important part of the plant carbon budget. The increased dark respiration, in the transgenics, is commensurate with higher carboxylic acid flux to the TCA cycle in these plants. The additional starch produced in *CA* overexpressers was only partly used in the dark by respiration, perhaps for increased growth with higher biomass, in agreement with the data of others (Biswal *et al.*, 2012; Ermakova *et al.*, 2019; Kandoi *et al.*, 2016; Lefebvre *et al.*, 2005).

Increases in overall biomass is important for obtaining high-yielding bioenergy crops (Ort *et al.*, 2015), where PSII photosynthetic efficiency, carbon assimilation, starch content, and dry matter accumulation have been shown to be high. Our results on transferring carbonic anhydrase from *Flaveria bidentis* to *Arabidopsis thaliana* have demonstrated a significant increase in carboxylic acids, amino acids, protein content, electron transport, carbon assimilation, starch content, and dry matter, which is in the right direction to meet the global needs ahead of us.

Experimental procedures

Sequence analysis

Homology search was made with basic local alignment search tool (BLAST), using Clustal W (http://www.ebi.ac.uk/Tools/msa/clustalo/), signal sequence predictions by Target P (http://www.cbs.dtu.dk/services/TargetP/), and nucleotide sequence data were from a web site: http://www.ncbi.nlm.nih.gov/.

Generation of transgenic and growth conditions

The full-length *FbβCA3* (accession no-AY167113) was cloned in pGEM-T Easy vector and subsequently in modified pCAMBIA1304 (Pattanayak and Tripathy, 2011), and then transformed in *Arabidopsis* using agrobacterium-mediated floral dip method (see Kandoi *et al.*, 2016, and Table S4). VC plants containing the null vector pCAMBIA1304 (i.e. without *FbβCA3* cDNA) were also generated and used for comparison with the transgenics since no significant differences in growth parameters were seen between the wild type (WT) and the VC plants.

Seeds of the transformed plants were screened on half-strength Murashige and Skoog (MS) agar medium containing 50 μg/mL kanamycin. Stratified *Arabidopsis* seeds were sown in agropeat: vermiculite (1:4) mixture in pots and grown under cool-white-fluorescent light (100 μmol photons m^{-2} s^{-1}), under 14-h light/10-h dark photoperiods, at 21 ± 1 °C. Plants' position was randomized, and the position of the trays rotated daily under the light.

Confirmation of transgenic lines by polymerase chain reaction (PCR) and Southern blot analysis

Genomic DNA was isolated by cetyl trimethyl ammonium bromide (CTAB) method (Nickrent, 1994) from four-week-old plants of the T1 generation. The presence of trans-gene in the plants was confirmed by PCR, using ^{35}S forward internal primer and *FbβCA3* reverse primer to ensure the incorporation of the whole cassette in sense orientation. The presence of *FbβCA3* transgene was analysed by Southern blot analysis. The genomic DNA from the leaves of the T3 generation of the vector control and the transgenic plants was digested with the restriction enzyme XbaI. The *nptII* coding sequence, amplified from the plasmid, was used for probe preparation, and labelled with (α^{32}P) dCTP, using a radioactive random primer labelling kit (Amersham-GE, UK). Southern blot was developed and used, as described by Sambrook and Russell (2001).

qRT-PCR

Relative expression of different genes was checked by using qRT-PCR on ABI Prism 7500 Sequence Detection System (Applied Biosystems, USA), and the design of the primers was based on sequence details (Table S5). Following the minimum information for publication of quantitative real-time PCR experiment (MIQE) guidelines (Bustin *et al*., 2009), all the details are provided in the supplementary material of our paper. The relative gene expression data were analysed using $2^{-\Delta\Delta C_t}$ quantification methods (Livak and Schmittgen, 2001; Taylor *et al*., 2019). Details of the procedure are also described in the supplementary material.

Western blot analysis

For immunoblot analysis, electrophoresis was carried out using 25 μg of plant protein, extracted from four-week-old leaves. Proteins were quantified by spectrophotometry, and Coomassie brilliant blue R250 methods were used for the visualization of proteins separated by SDS-PAGE. Separated proteins were blotted on nitrocellulose membranes (Towbin *et al*., 1979). The blots were probed using antibodies raised against the specific protein. To track the transfer efficiency of proteins in the blot lanes, reversible Ponceau staining was used because of its cost effectiveness (Sander *et al*., 2019). The rabbit anti-mouse IgG (1:20 000) conjugated to alkaline phosphatase (Sigma-Aldrich) was used as a secondary antibody. Blots were stained for alkaline phosphatase using 5-bromo-4-chloro-3-indolyl phosphate and nitro blue tetrazolium. Furthermore, polyclonal antibodies were used (for details, see Supplementary Table S6) for some major enzymes of Chl biosynthetic pathway. CA polyclonal antibody was raised in rabbits against epitope sequence TAQLQTLDSTKPGFDPVER and commercially prepared by Imgenx. This experiment was repeated three times.

CO_2 hydration activity

Leaf tissue (0.5 g) was homogenized with 1 mL buffer containing 40 mM HEPES-KOH (pH 8.0) and 10 mM dithiothreitol using chilled mortar and pestle (Hatch and Burnell, 1990). After adding an additional 1 mL of the buffer mixture, the homogenate was filtered through two layers of Miracloth. The filtrate was used for CA activity. The CO_2 hydration activity was determined using 6 ml of 20 mM Tris (pH 8.3) at 0 °C, 0.1 mL of enzyme extract, and 4 ml of ice-cold CO_2 saturated water. The activity was determined from the rate of pH shift from pH 8.3 to 6.3 and the rate was calculated as μmol CO_2 hydrated min^{-1} (mg Chl)$^{-1}$ by using the following equation:

$$\text{CA activity} = [2 \times (T_0 - T)]/[T \times \text{amount of Chl (mg)}],$$

where, T_0 and T are the times needed for the pH drop from 8.3 to 6.3 for both the non-enzymatic (inactivated at 95 °C) and the enzymatic reactions (Wilbur and Anderson, 1948). These experiments were performed using five biological replicates.

Estimation of chlorophyll, protein and free amino acids

Chl was extracted in 80% acetone, and its amount was estimated using the method of Porra *et al*. (1989), whereas the leaf soluble protein was measured as described by Bradford (1976). Free amino acids were analysed by the ninhydrin method, using leucine as a standard (Misra *et al*., 1975). These experiments were performed using 5 biological replicates.

PEPC activity

PEPC activity was measured in leaves of VC and *FbβCA3* overexpressor plants (see Supplementary Material for details). Enzyme-specific activity was expressed as μmol of NADH oxidized per mg of protein per hour. These experiments were performed using five biological replicates.

Whole-chain (WC), PSII, and PSI reactions

Thylakoid membranes were isolated in a buffer containing 0.01 M Tris and 1mM EDTA (pH 7.5). The homogenate was centrifuged at 12 000 ***g*** for 5 min and the pellet, containing thylakoid membranes, was suspended in a buffer containing 0.4 M sorbitol, 0.05 M Tris (pH 7.5), 1 mM $MgCl_2$, and 1 mM EDTA (Gupta and Tripathy, 2010; Jilani *et al*., 1996; Mohapatra and Tripathy, 2003). Using thylakoid membranes isolated from both VC and *CAx* plants, we monitored electron transport: (i) from water to methyl viologen [MV], involving both PSII and PSI; (ii) from water to phenylenediamine [PD], which measures only PSII; and (iii) from ascorbate/dichlorophenol-indophenol to MV, which measures only PSI. All the above measurements used a Clark-type oxygen electrode, as described by Chakraborty and Tripathy (1992). These experiments were performed using five biological replicates.

Determination of metabolite levels by GC-MS

For gas chromatography-mass spectrometry (GC-MS) analysis, polar metabolites were extracted with isopropanol: acetonitrile: water (3:3:2) mixture from 100 mg of complete rosettes ground previously to a fine powder. Metabolite samples were derivatized by methoxyamination, using a 20 mg/mL solution of methoxyamine hydrochloride in pyridine, and subsequent trimethylsilylation with N-Methyl-N-(trimethylsilyl) trifluoroacetamide (MSTFA). An aliquot of the derivate was injected into a GC-MS system (GCMS QP2010 Plus, Shimadzu). Signals were normalized to an internal standard molecule introduced into the samples (ribitol), allowing a relative quantification of the metabolites. Data sets presented were normalized to the wild-type control of each measured batch as a reference. These experiments were performed using three biological replicates.

Pulse-amplitude modulation (PAM) and Handy PEA measurements

Chl *a* fluorescence (for PSII activity) and transmission changes at 830 nm (for PSI activity) were measured simultaneously by the

Dual-PAM-100 system, using an automated ''Light Curve'' program from Walz (for details, see Yuan *et al*., 2014). These experiments were performed using five biological replicates. In addition, Chl *a* fluorescence induction was measured using Handy PEA (Plant Efficiency Analyzer), Hansatech Instruments, UK. For these measurements, *Arabidopsis* seedlings were pre-darkened for 20 min at room temperature (for details, see Kandoi *et al*., 2016, and references therein). These experiments were performed using eight biological replicates.

Carbon dioxide assimilation

Rates of CO_2 assimilation, at different light intensities (constant $[CO_2]$- 400 μmol mol^{-1}) as well as at constant light intensity (400 μmol photons m^{-2} s^{-1}), different $[CO_2]$ were measured using infrared gas analyzer, IRGA (LiCor 6400XT), with 6400-18A RGB (Red, Green, Blue) light source. During the experiments, the temperature of the chamber was maintained at 25 °C, and a relative humidity of 60%–70%. These experiments were performed using five biological replicates.

For the measurements of A/C_i curve (net CO_2 assimilation rate, A, versus calculated internal CO_2 concentration, C_i), humidified 2% O_2 and 98% N_2 was used; the carboxylation efficiency was obtained from the slope of the A/C_i curve (Li *et al*., 2009). Mesophyll conductance and chloroplastic CO_2 (Cc) were calculated using Thomas Sharkey's curve fitting model (Sharkey *et al*., 2007).

Starch content

For measuring the starch content, leaf samples were collected from three-week-old plants in the plant growth chamber immediately prior to the end of the light period. Samples were digested with perchloric acid, and then the starch was assayed spectrophotometrically, using anthrone, a colour reagent (Rose *et al*., 1991). These experiments were performed using five biological replicates.

Statistical analysis

All the details for this analysis are described in the Supplementary Material.

Acknowledgments

This work was supported by the Department of Science and Technology (#DST-SERB-EMR/2016/004976), Department of Biotechnology (#BT/PR11896/BPA/118/3/2014), Government of India, National Agriculture Innovation Project (#PAC-SLS-BCT-NAIP-09080312-371) from the ICAR, and BSR Faculty Fellowship to BCT, and by the D.S. Kothari Post-Doctoral Fellowship (BL/19-20/0157) to DK from the University Grants Commission, Government of India. We thank Alexandrina Stirbet from Virginia, USA, for her generous help in the calculation of some of the data.

Conflict of interest

There is no known conflict of interest.

Author contributions

BCT planned and designed the experiments; DK, KR performed the experiments, and analysed the data; BCT, DK, GG and KR wrote the manuscript.

Data availability statement

The data that support the findings of this study are available from the corresponding author upon request.

References

Ainsworth, E.A. and Long, S.P. (2005) What have we learned from 15 years of free air CO_2 enrichment (FACE)? A meta-analytic review of the responses of photosynthesis, canopy properties and plant production to rising CO_2. *New Phytol.* **165**, 351–372.

Badger, M.R. and Price, G.D. (1994) The role of carbonic anhydrase in photosynthesis. *Annu. Rev. Plant Physiol. Plant Mol. Biol.* **45, 1**, 369–392.

Baker, N.R. (2008) Chlorophyll fluorescence: a probe of photosynthesis in vivo. *Annu. Rev. Plant Biol.* **59**, 89–113.

Baker, N.R., Harbinson, J. and Kramer, D.M. (2007) Determining the limitations and regulation of photosynthetic energy transduction in leaves. *Plant Cell Environ.* **30**, 1107–1125.

Bernacchi, C.J., Bagley, J.E., Serbin, S.P., RuizVera, U.M., Rosenthal, D.M. and Vanloocke, A. (2013) Modelling C_3 photosynthesis from the chloroplast to the ecosystem. *Plant Cell Environ.* **36**, 1641–1657.

Bernacchi, C.J., Singsaas, E.L., Pimentel, C., Portis, A.R. Jr and Long, S.P. (2001) Improved temperature response functions for models of Rubisco-limited photosynthesis. *Plant Cell Environ.* **24**, 253–260.

Biswal, A.K., Pattanayak, G.K., Pandey, S.S., Leelavathi, S., Reddy, V.S., Govindjee, [G.] and Tripathy, B.C. (2012) Light intensity-dependent modulation of chlorophyll *b* biosynthesis and photosynthesis by overexpression of chlorophyllide *a* oxygenase in tobacco. *Plant Physiol.* **159**, 433–449.

Bonacci, W., Teng, P.K., Afonso, B., Niederholtmeyer, H., Grob, P., Silver, P.A. and Savage, D.F. (2012) Modularity of a carbon-fixing protein organelle. *Proc. Natl Acad. Sci. USA*, **109**, 478–483.

Borba, A.R., Serra, T.S., Gorska, A., Gouveia, P., Cordeiro, A.M., Reyna-Llorens, I., Knerova, J. *et al*. (2018) Synergistic binding of bHLH transcription factors to the promoter of the maize NADP-ME gene used in C4 photosynthesis is based on an ancient code found in the ancestral C3 state. *Mol. Biol. Evol.* **35**, 1690–1705.

Bradford, M.M. (1976) A rapid and sensitive method for the quantitation of microgram quantities of protein utilizing the principle of protein-dye binding. *Anal. Biochem.* **72**, 248–254.

Burke, J.J. (1990) High temperature stress and adaptation in crops. In *Stress Response in Plants: Adaptation and Acclimation Mechanisms* (Alscher, R.G. and Cummings, J.R., eds), pp. 295–309. New York, NY: Wiley-Liss.

Bustin, S.A., Benes, V., Garson, J.A., Hellemans, J., Huggett, J., Kubista, M., Mueller, R. *et al*. (2009) The MIQE guidelines: minimum information for publication of quantitative real-time PCR experiments. *Clin. Chem.* **55**, 611–622.

Chakraborty, N. and Tripathy, B.C. (1992) 5-aminolevulinic acid-induced photodynamic reactions in thylakoid membranes of cucumber (*Cucumis sativus* L.) cotyledons. *J. Plant Biochem. Biotech.* **1**, 65–68.

Cousins, A.B., Badger, M.R. and von Caemmerer, S. (2006) A transgenic approach to understanding the influence of carbonic anhydrase on $C^{18}OO$ discrimination during C4 photosynthesis. *Plant Physiol.* **142**, 662–672.

Dąbrowska-Bronk, J., Komar, D.N., Rusaczonek, A., Kozłowska-Makulska, A., Szechyńska-Hebda, M. and Karpiński, S. (2016) β-carbonic anhydrases and carbonic ions uptake positively influence Arabidopsis photosynthesis, oxidative stress tolerance and growth in light dependent manner. *J. Plant Physiol.* **203**, 44–54.

Daniell, H., Lee, S.B., Panchal, T. and Wiebe, P.O. (2001) Expression of cholera toxin B subunit gene and assembly as functional oligomers in transgenic tobacco chloroplasts. *J. Mol. Biol.* **311**, 1001–1009.

DiMario, R.J., Clayton, H., Mukherjee, A., Ludwig, M. and Moroney, J.V. (2017) Plant carbonic anhydrases: structures, locations, evolution, and physiological roles. *Mol. Plant*, **10**, 30–46.

DiMario, R.J., Machingura, M.C., Waldrop, G.L. and Moroney, J.V. (2018) The many types of carbonic anhydrases in photosynthetic organisms. *Plant Sci.* **268**, 11–17.

DiMario, R.J., Quebedeaux, J.C., Longstreth, D.J., Dassanayake, M., Hartman, M.M. and Moroney, J.V. (2016) The cytoplasmic carbonic anhydrases βCA2 and βCA4 are required for optimal plant growth at low CO_2. *Plant Physiol.* **171**, 280–293.

Ermakova, M., Lopez-Calcagno, P.E., Raines, C.A., Furbank, R.T. and von Caemmerer, S. (2019) Overexpression of the Rieske FeS protein of the Cytochrome b6f complex increases C_4 photosynthesis in Setaria viridis. *Commun. Biol.* **2**, 1–12.

Ferreira, F.J., Guo, C. and Coleman, J.R. (2008) Reduction of plastid-localized carbonic anhydrase activity results in reduced arabidopsis seedling survivorship. *Plant Physiol.* **147**, 585–594.

Flemetakis, E., Dimou, M., Cotzur, D., Aivalakis, G., Efrose, R.C., Kenoutis, C., Udvardi, M. *et al*. (2003) A *Lotus japonicus β*-type carbonic anhydrase gene expression pattern suggests distinct physiological roles during nodule development. *Biochem. Biophys. Acta*, **1628**, 186–194.

Flexas, J., Bota, J., Loreto, F., Cornic, G. and Sharkey, T.D. (2008) Diffusive and metabolic limitations to photosynthesis under drought and salinity in C3 plants. *Plant Biol.* **6**, 269–279.

Flexas, J., Niinemets, U., Gallé, A., Barbour, M.M., Centritto, M., Diaz-Espejo, A., Douthe, C. *et al*. (2013) Diffusional conductances to CO_2 as a target for increasing photosynthesis and photosynthetic water-use efficiency. *Photosynth. Res.* **117**, 45–59.

Flexas, J., Ortuño, M.F., Ribas-Carbo, M., Diaz-Espejo, A., Flórez-Sarasa, I.D. and Medrano, H. (2007) Mesophyll conductance to CO2 in *Arabidopsis thaliana*. *New Phytol.* **175**, 501–511.

Floryszak-Wieczorek, J. and Arasimowicz-Jelonek, M. (2017) The multifunctional face of plant carbonic anhydrase. *Plant Physiol. Biochem.* **112**, 362–368.

Garai, S. and Tripathy, B.C. (2018) Alleviation of nitrogen and sulfur deficiency and enhancement of photosynthesis in *Arabidopsis thaliana* by overexpression of Uroporphyrinogen III Methyltransferase (UPM1). *Front. Plant Sci.*, **9**, # 1365.

Genty, B., Goulas, Y., Dimon, B., Peltier, G., Briantais, J.M. and Moya, I. (1992) Modulation of efficiency of primary conversion in leaves, mechanisms involved at PS 2. In *Research in Photosynthesis*, vol. **IV** (Murata, N., ed), pp. 603–610. Dordrecht: Kluwer Academic Publishers.

Groszmann, M., Osborn, H.L. and Evans, J.R. (2017) Carbon dioxide and water transport through plant aquaporins. *Plant Cell Environ.* **40**, 938–961.

Gupta, V. and Tripathy, B.C. (2010) Effect of light quality on chlorophyll accumulation and protein expression in wheat (*Triticum aestivum* L.) seedlings. *Intern. J. Biotech. Biochem.* **6**, 521–537.

Hamdani, S., Qu, M., Xin, C.-P., Li, M., Chu, C., Govindjee, [G.] and Zhu, X.-G. (2015) Variations between the photosynthetic properties of elite and landrace Chinese rice cultivars revealed by simultaneous measurements of 820 nm transmission signal and chlorophyll a fluorescence induction. *J. Plant Physiol.* **177**, 128–138.

Hatch, M.D. and Burnell, J.N. (1990) Carbonic anhydrase activity in leaves and its role in the first step of C-4 photosynthesis. *Plant Physiol.* **93**, 825–828.

Hewett-Emmett, D. and Tashian, R.E. (1996) Functional diversity, conservation, and convergence in the evolution of the α-, β-, and γ-carbonic anhydrase gene families. *Mol. Phylogen. Evol.* **5**, 50–77.

Hines, K.M., Chaudhari, V., Edgeworth, K.N., Owens, T.G. and Hanson, M.R. (2021) Absence of carbonic anhydrase in chloroplasts affects C_3 plant development but not photosynthesis. *Proc. Natl Acad. Sci. USA*, **118**, e2107425118.

Hoang, C.V. and Chapman, K.D. (2002) Biochemical and molecular inhibition of plastidial carbonic anhydrase reduces the incorporation of acetate into lipids in cotton embryos and tobacco cell suspensions and leaves. *Plant Physiol.* **128**, 1417–1427.

Hu, H., Boisson-Dernier, A., Israelsson-Nordström, M., Böhmer, M., Xue, S., Ries, A., Godoski, J. *et al*. (2010) Carbonic anhydrases are upstream regulators of CO_2-controlled stomatal movements in guard cells. *Nat. Cell Biol.* **12**, 87–93.

Ignatova, L.K., Moskvin, O.V., Romanova, A.K. and Ivanov, B.N. (1998) Carbonic anhydrases in the C3 -plant leaf cell Aust. *J. Plant Physiol.* **25**, 673–677.

Jacob, J., Greitner, C. and Drake, B.G. (1995) Acclimation of photosynthesis in relation to RuBisco and non-structural carbohydrate contents and in situ carboxylase activity in *Scirpus olneyi* grown at elevated CO_2 in the field. *Plant Cell Environ.* **18**, 875–884.

Jeanjean, R., Latifi, A., Matthijs, H.C. and Havaux, M. (2008) The PsaE subunit of Photosystem I prevents light-induced formation of reduced oxygen species in the cyanobacterium *Synechocystis* sp. PCC 6803. *Biochim. Biophys. Acta*, **1777**, 308–316.

Jilani, A., Kar, S., Bose, S. and Tripathy, B.C. (1996) Regulation of the carotenoid content and chloroplast development by levulinic acid. *Physiol. Plant*, **96**, 139–145.

Jiménez-Francisco, B., Stirbet, A., Aguado-Santacruz, G.A., Campos, H., Conde-Martínez, F.V., Padilla-Chacón, D., Trejo, C. *et al*. (2020) A comparative chlorophyll a fluorescence study on isolated cells and intact leaves of *Bouteloua gracilis* (blue grama grass). *Photosynthetica*, **58**, 262–274.

Kandoi, D., Mohanty, S., Govindjee, [G.] and Tripathy, B.C. (2016) Towards efficient photosynthesis: overexpression of *Zea mays* phosphoenolpyruvate carboxylase in *Arabidopsis thaliana*. *Photosynth. Res.* **130**, 47–72.

Kandoi, D., Mohanty, S. and Tripathy, B.C. (2018) Overexpression of plastidic maize NADP-malate dehydrogenase (ZmNADP-MDH) in *Arabidopsis thaliana* confers tolerance to salt stress. *Protoplasma*, **255**, 547–563.

Kavroulakis, N., Flemetakis, E., Aivalakis, G. and Katinakis, P. (2000) Carbon metabolism in developing soybean root nodules: the role of carbonic anhydrase. *Mol. Plant Microbe*, **22**, 13–14.

Kolbe, A.R., Brutnell, T.P., Cousins, A.B. and Studer, A.J. (2018) Carbonic anhydrase mutants in *Zea mays* have altered stomatal responses to environmental signals. *Plant Physiol.* **177**, 980–989.

Krause, G.H. and Weis, E. (1991) Chlorophyll fluorescence and photosynthesis: the basics. *Annu. Rev. Plant Physiol. Plant Mol. Biol.* **42**, 313–349.

Lee, S.B., Kwon, H.B., Kwon, S.J., Park, S.C., Jeong, M.J., Han, S.E., Byun, M.O. *et al*. (2003) Accumulation of trehalose within transgenic chloroplasts confers drought tolerance. *Mol. Breeding*, **11**, 1–13.

Lefebvre, S., Lawson, T., Fryer, M., Zakhleniuk, O.V., Lloyd, J.C. and Raines, C.A. (2005) Increased sedoheptulose-1,7-bisphosphatase activity in transgenic tobacco plants stimulates photosynthesis and growth from an early stage in development. *Plant Physiol.* **138**, 451–460.

Li, Y., Gao, Y., Xu, X., Shen, Q. and Guo, S. (2009) Light saturated photosynthetic rate in high-nitrogen rice (*Oryza sativa* L.) leaves is related to chloroplast CO_2 concentration. *J. Exp. Bot.* **60**, 2351–2360.

Liljas, A. and Laurberg, M. (2000) A wheel invented three times: the molecular structures of the three carbonic anhydrases. *EMBO J.* **1**, 16–17.

Lin, H.C., Arrivault, S., Coe, R.A., Karki, S., Covshoff, S., Bagunu, E., Lunn, J.E. *et al*. (2020) A partial C_4 photosynthetic biochemical pathway in rice. *Front. Plant Sci.* **11**, 1581.

Lindskog, S. (1997) Structure and mechanism of carbonic anhydrase. *Pharmacol. Ther.* **74**, 1–20.

Livak, K.J. and Schmittgen, T.D. (2001) Analysis of relative gene expression data using real-time quantitative PCR and the $2^{-\Delta\Delta CT}$ method. *Methods*, **25**, 402–408.

Long, S.P., Marshall-Colon, A. and Zhu, X.-G. (2015) Meeting the global food demand of the future by engineering crop photosynthesis and yield potential. *Cell*, **161**, 56–66.

Lu, Y.K., Theg, S.M. and Stemler, A.J. (2005) Carbonic anhydrase activity of the Photosystem II OEC33 protein from pea. *Plant Cell Physiol.* **46**, 1944–1953.

Ludwig, M. (2012) Carbonic anhydrase and the molecular evolution of C4 photosynthesis. *Plant Cell Environ.* **35**, 22–37.

Majeau, N., Arnoldo, M.A. and Coleman, J.R. (1994) Modification of carbonic anhydrase activity by antisense and over-expression constructs in transgenic tobacco. *Plant Mol Biol.* **25**, 377–385.

Majeau, N. and Coleman, J.R. (1994) Correlation of carbonic anhydrase and ribulose-1,5-bisphosphate carboxylase/oxygenase expression in pea. *Plant Physiol.* **104**, 1393–1399.

Makino, A., Nakano, H. and Mae, T. (1994) Responses of ribulose-1,5-bisphosphate carboxylase, cytochrome *f* and sucrose synthesis enzymes in rice leaves to leaf nitrogen and their relationships to photosynthesis. *Plant Physiol.* **105**, 173–179.

Malkin, S. and Kok, B. (1966) Fluorescence induction studies in isolated chloroplasts. I. Number of components involved in the reaction and quantum yields. *Biochim. Biophys. Acta*, **126**, 413–432.

Manter, D.K. and Kerrigan, J. (2004) A/C(i) curve analysis across a range of woody plant species: Influence of regression analysis parameters and mesophyll conductance. *J. Exp. Bot.* **55**, 2581–2588.

Masumoto, C., Miyazawa, S., Ohkawa, H., Fukuda, T., Taniguchi, Y., Murayama, S., Kusano, M. *et al*. (2010) Phosphoenolpyruvate carboxylase intrinsically located in the chloroplast of rice plays a crucial role in ammonium assimilation. *Proc Natl Acad Sci USA*, **107**, 5226–5231.

Melzer, E. and O'Leary, M.H. (1987) Anapleurotic CO_2 fixation by phosphoenolpyruvate carboxylase in C_3 plants. *Plant Physiol.* **84**, 58–60.

Misra, P.S., Mertz, E.T. and Glover, D.V. (1975) Studies on corn proteins: VIII. Free amino acid content of opaque-2 and double mutants. *Cereal Chem.* **52**, 844–848.

Miyao, M., Masumoto, C., Miyazawa, S. and Fukayama, H. (2011) Lessons from engineering a single-cell C(4) photosynthetic pathway into rice. *J. Exp. Bot.* **62**, 3021–3029.

Mohapatra, A. and Tripathy, B.C. (2003) Developmental changes in sub-plastidic distribution of chlorophyll biosynthetic intermediates in Cucumber (*Cucumis sativus* L.). *J. Plant Physiol.* **160**, 9–15.

Momayyezi, M., McKown, A.D., Bell, S.C.S. and Guy, R.D. (2020) Emerging roles for carbonic anhydrase in mesophyll conductance and photosynthesis. *Plant J.* **101**, 831–844.

Moroney, J.V., Bartlett, S.G. and Samuelsson, G. (2001) Carbonic anhydrases in plants and algae. *Plant Cell Environ.* **24**, 141–153.

Moroney, J.V., Ma, Y., Frey, W.D., Fusilier, K.A., Pham, T.T., Simms, T.A., DiMario, R.J. *et al*. (2011) The carbonic anhydrase isoforms of *Chlamydomonas reinhardtii:* intracellular location, expression, and physiological roles. *Photosynth. Res.* **109**, 133–149.

Nickrent, D.L. (1994) From field to film: Rapid sequencing methods for field-collected plant species. *Biotechniques*, **16**, 470–475.

Ogée, J., Wingate, L. and Genty, B. (2018) Estimating mesophyll conductance from measurements of $C^{18}OO$ photosynthetic discrimination and carbonic anhydrase activity. *Plant Physiol.* **178**, 728–752.

Okabe, K., Yang, S.-Y., Tsuzuki, M. and Miyachi, S. (1984) Carbonic anhydrase: Its content in spinach leaves and its taxonomic diversity studied with anti-spinach leaf carbonic anhydrase antibody. *Plant Sci. Lett.* **33**, 145–153.

Ort, D.R., Merchant, S.S., Alric, J., Barkan, A., Blankenship, R.E., Bock, R., Croce, R. *et al*. (2015) Redesigning photosynthesis to sustainably meet global food and bioenergy demand. *Proc. Natl. Acad. Sci. USA*, **112**, 8529–8536.

Osborn, H.L., Alonso-Cantabrana, H., Sharwood, R.E., Covshoff, S., Evans, J.R., Furbank, R.T. and von Caemmerer, S. (2017) Effects of reduced carbonic anhydrase activity on CO_2 assimilation rates in *Setaria viridis*: a transgenic analysis. *J. Exp. Bot.* **68**, 299–310.

Pal, A. and Borthakur, D. (2015) Transgenic overexpression of Leucaena β-carbonic anhydrases in tobacco does not affect carbon assimilation and overall biomass. *Plant Biosyst.* **150**, 1–10.

Papageorgiou, G.C. and Govindjee, [G.] (eds). (2004) *Chlorophyll a* Fluorescence: A Signature of Photosynthesis. Dordrecht, The Netherlands: Springer. ISBN: 978-1-4020-3217-2.

Pattanayak, G.K. and Tripathy, B.C. (2011) Overexpression of protochlorophyllide oxidoreductase c regulates oxidative stress in *Arabidopsis*. *PLoS One*, **6**, e26532.

Pocker, Y. and Ng, J.S.Y. (1973) Plant carbonic anhydrase: properties and carbon dioxide hydration kinetics. *Biochemistry*, **12**, 5127–5134.

Porra, R.J., Thompson, W.A. and Kriedemann, P.E. (1989) Determination of accurate extinction coefficients and simultaneous-equations for assaying chlorophyll-a and chlorophyll-b extracted with 4 different solvents - Verification of the concentration of chlorophyll standards by atomic absorption spectroscopy. *Biochim. Biophys. Acta*, **975**, 384–394.

Poschenrieder, C., Fernández, J.A., Rubio, L., Pérez, L., Terés, J. and Barceló, J. (2018) Transport and use of bicarbonate in plants: current knowledge and challenges ahead. *Int. J. Mol. Sci.* **19**, 1352.

Price, G.D., von Caemmerer, S., Evans, J.R., Yu, J.-W., Lloyd, J., Oja, V., Kell, P. *et al*. (1994) Specific reduction of chloroplast carbonic anhydrase activity by antisense RNA in transgenic tobacco plants has a minor effect on photosynthetic CO2 assimilation. *Planta*, **193**, 331–340.

Raven, J.A. (1997) Inorganic carbon acquisition by marine autotrophs. *Adv. Bot. Res.* **27**, 85–209.

Rose, R., Rose, C.L., Omi, S.K., Forry, K.R., Durall, D.M. and Bigg, W.L. (1991) Starch determination by perchloric acid vs enzymes: evaluating the accuracy and precision of six colorimetric methods. *J. Agric. Food Chem.* **39**, 2–11.

Sambrook, J. and Russell, D.W. (2001) *Molecular Cloning: A Laboratory Manual*, 3rd ed. New York: Cold Spring Harbor Laboratory Press.

Sander, H., Wallace, S., Plouse, R., Tiwari, S. and Gomes, A.V. (2019) Ponceau S waste: Ponceau S staining for total protein normalization. *Anal Biochem.* **575**, 44–53.

Schuler, M.L., Mantegazza, O. and Weber, A.P. (2016) Engineering C4 photosynthesis into C3 chassis in the synthetic biology age. *Plant J.* **87**, 51–65.

Sen, P., Ghosh, S., Sarkar, S.N., Chanda, P., Mukherjee, A., Datta, S.K. and Datta, K. (2017) Pyramiding of three C4 specific genes towards yield enhancement in rice. *Plant Cell Tissue Organ Cult.* **128**, 145–160.

Sharkey, T.D. (1985) O_2-insensitive photosynthesis in C_3 plants: Its occurrence and a possible explanation. *Plant Physiol.* **78**, 71–75.

Sharkey, T.D., Bernacchi, C.J., Farquhar, G.D. and Singsaas, E.L. (2007) Fitting photosynthetic carbon dioxide response curves for C3 leaves. *Plant Cell Environ.* **30**, 1035–1040.

Sharp, R.E., Matthews, M.A. and Boyer, J.S. (1984) Kok effect and the quantum yield of photosynthesis. *Plant Physiol.* **75**, 95–101.

Shevela, D., Eaton-Rye, J.J., Shen, J.R. and Govindjee, [G.] (2012) Photosystem II and the unique role of bicarbonate: a historical perspective. *Biochim. Biophys. Acta*, **1817**, 1134–1151.

Shitov, A.V., Terentyev, V.V., Zharmukhamedov, S.K., Rodionova, M.V., Karacan, M., Karacan, N., Klimov, V.V. *et al*. (2018) Is carbonic anhydrase activity of Photosystem II required for its maximum electron transport rate? *Biochim. Biophys. Acta Bioenerg.* **1859**, 292–299.

Simkin, A.J., McAusland, L., Lawson, T. and Raines, C.A. (2017) Overexpression of the Rieske FeS protein increases electron transport rates and biomass yield. *Plant Physiol.* **175**, 134–145.

Soda, N., Gupta, B.K., Anwar, K., Sharan, A., Govindjee, [G.], Singla-Pareek, S.L. and Pareek, A. (2018) Rice intermediate filament, OsIF, stabilizes photosynthetic machinery and yield under salinity and heat stress. *Sci. Rep.* **8**, 4072.

Stemler, A.J. (1997) The case for chloroplast thylakoid carbonic anhydrase. *Physiol. Plant*, **99**, 348–353.

Taylor, S.C., Nadeau, K., Abbasi, M., Lachance, C., Nguyen, M. and Fenrich, J. (2019) The ultimate qPCR experiment: producing publication quality, reproducible data the first time. *Trends Biotechnol.* **37**, 761–774.

Tobin, A.J. (1970) Carbonic anhydrase from parsley leaves. *J. Biol. Chem.* **215**, 2656–2666.

Towbin, H., Staehelin, T. and Gordon, J. (1979) Electrophoretic transfer of proteins from polyacrylamide gels to nitrocellulose sheets: procedure and some applications. *Proc. Natl Acad. Sci. USA*, **76**, 4350–4354.

Tsimilli-Michael, M., Eggenberg, P., Biro, B., Köves-Pechy, K., Vörös, I. and Strasser, R.J. (2000) Synergistic and antagonistic effects of arbuscular mycorrhizal fungi and *Azospirillum* and *Rhizobium* nitrogen-fixers on the photosynthetic activity of alfalfa, probed by the polyphasic chlorophyll a fluorescence transient O-J-I-P. *Appl. Soil Ecol.* **15**, 169–182.

Tsuzuki, M., Miyachi, S. and Edwards, G. (1985) Localization of carbonic anhydrase in mesophyll cells of terrestrial C3 plants in relation to CO_2 assimilation. *Plant Cell Physiol.* **26**, 881–891.

Tyerman, S.D., Niemietz, C.M. and Bramley, H. (2002) Plant aquaporins: multifunctional water and solute channels with expanding roles. *Plant Cell Environ.* **25**, 173–194.

von Caemmerer, S. and Farquhar, G.D. (1981) Some relationships between the biochemistry of photosynthesis and the gas exchange of leaves. *Planta*, **153**, 376–387.

von Caemmerer, S., Quinn, V., Hancock, N.C., Price, G.D., Furbank, R.T. and Ludwig, M. (2004) Carbonic anhydrase and C_4 photosynthesis: a transgenic analysis. *Plant Cell Environ.* **27**, 697–703.

Wilbur, K.M. and Anderson, N.G. (1948) Electrometric and colorimetric determination of carbonic anhydrase. *J. Biol. Chem.* **176**, 147–154.

Yuan, X., Zhang, L., Ning, N., Wen, Y., Dong, S., Yin, M., Guo, M. *et al*. (2014) Photosynthetic physiological response of Radix isatidis (*Isatis indigotica* Fort.) seedlings to nicosulfuron. *PLoS One*, **9**, e105310.

Supporting information

Additional supporting information may be found online in the Supporting Information section at the end of the article.

Figure S1 Comparison of the amino acid sequences of *AtβCAs* with *FbβCA3* (cytoplasmic carbonic anhydrase, *CA*).
Figure S2 Confirmation of *Flaveria bidentis CA* overexpressed plants (a): PCR reaction was performed with genomic DNA isolated from different transgenic lines of T1 generation plants by using ^{35}S internal forward primer and gene specific reverse primer; (b): Genomic DNA of vector control and T1 generation of *CAx* plants, having resistance to *nptII*, were used as template and PCR of *nptII* was done by using *nptII* primers; (c): Southern blotting using *npt II* as a probe.
Figure S3 *PEPC* enzymatic activity *in vitro*; the activity of *PEPC* in the transgenics was similar to that in the vector control plants (~3 μmol/mg protein/h).
Figure S4 RNA denaturing agarose gel electrophoresis of VC and several transgenics.
Figure S5 Immunoblot analysis of LHCII and LSU of rubisco in the vector control and the two transgenics CAx3 and CAx5 (a) LHCII; (b) rubisco large subunit (LSU).
Table S1 Score of pairwise alignment of different sequences of *Arabidopsis thaliana βCA* with *Flaveria bidentis βCA3* (258 amino acids) and localization of these isoforms.
Table S2 Chlorophyll *a* fluorescence measurements of VC and *CAx* plants grown in soil.
Table S3 Morphological parameters of the transgenics and the vector control plants.
Table S4 Primers used for cloning.
Table S5 Primers used for RT-qPCR analysis.
Table S6 Antibodies used in this study.

